

1 Inferring the seasonal dynamics and abundance 2 of an invasive species using a spatio-temporal 3 stacked machine learning model 4

5 Daniele Da Re^{1,2}, Giovanni Marini^{2,3}, Carmelo Bonannella^{4,5}, Fabrizio Laurini⁶, Mattia
6 Manica^{3,7}, Nikoleta Anicic⁸, Alessandro Albieri⁹, Paola Angelini¹⁰, Daniele Arnoldi², Federica
7 Bertola¹¹, Beniamino Caputo¹², Claudio De Liberato¹³, Alessandra della Torre¹², Eleonora
8 Flacio⁸, Alessandra Franceschini¹⁴, Francesco Gradoni¹⁵, Përparim Kadriaj¹⁶, Valeria
9 Lencioni¹⁴, Irene Del Lesto¹³, Francesco La Russa¹⁷, Riccardo Paolo Lia¹⁸, Fabrizio
10 Montarsi¹⁵, Domenico Otranto¹⁸, Gregory L'Ambert¹⁹, Anna Paola Rizzoli^{2,3}, Pasquale
11 Rombolà¹³, Federico Romiti¹³, Gionata Stancher¹¹, Alessandra Torina¹⁷, Enkelejda Velo¹⁶,
12 Chiara Virgillito¹², Fabiana Zandonai¹¹, Roberto Rosà^{1,2}

13
14 ¹Center Agriculture Food Environment, University of Trento, San Michele all'Adige, Italy

15 ²Research and Innovation Centre, Fondazione Edmund Mach, San Michele all'Adige, Italy

16 ³Epilab-JRU, FEM-FBK Joint Research Unit, Province of Trento, Italy

17 ⁴OpenGeoHub Foundation, Wageningen, The Netherlands

18 ⁵Laboratory of Geo-Information Science and Remote Sensing, Wageningen University &
19 Research, Wageningen, The Netherlands

20 ⁶University of Parma, Parma, Italy

21 ⁷Bruno Kessler Foundation, Trento, Italy

22 ⁸Institute of Microbiology, University of Applied Sciences and Arts of Southern Switzerland
23 (SUPSI), Mendrisio, Switzerland

24 ⁹Centro Agricoltura Ambiente "G.Nicoli", Crevalcore, Italy

25 ¹⁰Emilia Romagna region, Bologna, Italy

26 ¹¹Fondazione Museo Civico di Rovereto, Rovereto, Italy

27 ¹²La Sapienza University, Rome, Italy

28 ¹³Istituto Zooprofilattico Sperimentale del Lazio e della Toscana "M. Aleandri", Italy

29 ¹⁴MUSE - Museo delle Scienze, Trento, Italy

30 ¹⁵Istituto Zooprofilattico Sperimentale delle Venezie, Padua, Italy

31 ¹⁶Institute of Public Health, Tirana, Albania

32 ¹⁷Istituto Zooprofilattico Sicily, Palermo, Italy

33 ¹⁸University of Bari, Bari, Italy

34 ¹⁹EID Méditerranée, Montpellier, France

35
36 Corresponding author: Daniele Da Re, daniele.dare@unitn.it

37 Abstract

38 Various modelling techniques are available to understand the temporal and spatial variations
39 of the phenology of species. Scientists often rely on correlative models, which establish a
40 statistical relationship between a response variable (such as species abundance or
41 presence-absence) and a set of predominantly abiotic covariates. The modelling approach
42 choice, i.e. the algorithm, is a crucial factor for addressing the multiple sources of variability
43 that can lead to disparate outcomes when different models are applied to the same dataset.
44 This inter-model variability has led to the adoption of ensemble modelling techniques, among
45 which stacked generalisation, which has recently demonstrated its capacity to produce
46 robust results. Stacked ensemble modelling incorporates predictions from multiple base
47 learners or models as inputs for a meta-learner. The meta-learner, in turn, assimilates these
48 predictions and generates a final prediction by combining the information from all the base
49 learners. In our study, we utilized a recently published dataset documenting egg abundance
50 observations of *Aedes albopictus* collected using ovitraps. This dataset spans various
51 locations in southern Europe, covering four countries - Albania, France, Italy, and
52 Switzerland - and encompasses multiple seasons from 2010 to 2022. Utilising these ovitrap
53 observations and a set of environmental predictors, we employed a stacked machine
54 learning model to forecast the weekly average number of mosquito eggs. This approach
55 enabled us to i) unearth the seasonal dynamics of *Ae. albopictus* for 12 years; ii) generate
56 spatio-temporal explicit forecasts of mosquito egg abundance in regions not covered by
57 conventional monitoring initiatives. Beyond its immediate application for public health
58 management, our work presents a versatile modelling framework adaptable to infer the
59 spatio-temporal abundance of various species, extending its relevance beyond the specific
60 case of *Ae. albopictus*.

61

62 Keywords

63 Arthropod, *Aedes albopictus*, forecast, invasive species, population dynamics, time-series.

64 Author Contributions

65 Daniele Da Re, Beniamino Caputo, Alessandra della Torre and Roberto Rosà conceived the
66 study; Daniele Da Re and Roberto Rosà designed the methodology, with relevant
67 contributions from Carmelo Bonannella, Giovanni Marini, Fabrizio Laurini and Mattia Manica;
68 Nikoleta Anicic, Alessandro Albieri, Paola Angelini, Daniele Arnoldi, Federica Bertola,
69 Beniamino Caputo, Claudio De Liberato, Enkelejda Velo, Eleonora Flacio, Alessandra
70 Franceschini, Perparim Kadriaj, Valeria Lencioni, Irene Del Lesto, Francesco La Russa,
71 Riccardo Paolo Lia, Fabrizio Montarsi, Francesco Gradoni, Gregory L'Ambert, Federico
72 Romiti, Gionata Stancher, Fabiana Zandonai collected the data; Daniele Da Re, Carmelo
73 Bonannella, Giovanni Marini, Fabrizio Laurini, Mattia Manica and Roberto Rosà analysed the
74 data; Daniele Da Re led the writing of the manuscript. All authors contributed critically to the
75 drafts and gave final approval for publication.

76

77 Acknowledgements

78 The study was supported by the Italian Ministry of University and Research (MUR)
79 PRIN2020 "Tackling mosquitoes in Italy: from citizen to bench and back" (N. 2020XYBN88).
80 This study was partially funded by EU grant 874850 MOOD and is catalogued as MOOD
81 098. This study was partially supported by EU funding within the MUR PNRR Extended
82 Partnership initiative on Emerging Infectious Diseases (Project no. PE00000007, INF-ACT).
83 The contents of this publication are the sole responsibility of the authors and don't
84 necessarily reflect the views of the European Commission. Gionata Stancher and Federica
85 Bertola thank the municipalities belonging to Comunità della Vallagarina and Comunità Alto
86 Garda e Ledro. Monitoring activities in Trento were financed by the Trento Municipality.

87 1. Introduction

88 Understanding the phenology of species, the study of periodic events in biological life
89 cycles influenced by seasonal and annual climate fluctuations, is of paramount importance
90 across various domains such as agriculture (e.g., for crop yield forecasts; Fand et al., 2014),
91 nature conservation (e.g., for assessing species responses to global changes; Ettinger,
92 Chamberlain, and Wolkovich, 2022), and addressing public health concerns related to
93 allergens and emerging infectious diseases carried by arthropod vectors (Burkett-Cadena et
94 al., 2011). Ecologists have therefore developed and tested several modelling approaches,
95 i.e. the mechanistic and correlative approaches, to infer the phenology of species and how it
96 varies over space and time. The mechanistic approach employs laboratory or field
97 observations about the influence of biotic or abiotic factors on the targeted life history traits
98 (e.g. the effect of temperature on a juvenile form development rate) to parametrise
99 mathematical models inferring the life cycle of the species of interest (e.g. Tran et al., 2013;
100 Marini et al., 2019; Pfab et al., 2018; Da Re et al., 2022). Although generally accurate,
101 mechanistic models often require estimating multiple parameters, constrained by the
102 availability of ecological observations in the scientific literature (Tjaden et al., 2013; Da Re et
103 al., 2022). As an alternative, ecologists frequently turn to correlative models, which establish
104 statistical relationships between a response variable (e.g., species abundance or presence-
105 absence) and a set of mostly abiotic covariates (Guisan et al., 2017; Edwards and Crone,
106 2021).

107 Despite the utility of correlative models, their outputs are subject to various sources
108 of variability, such as sampling location bias and model tuning (Hortal et al., 2008; Fourcade
109 2021; Bazzichetto et al., 2023; Da Re et al., 2023a). The choice of modelling method, in
110 particular, has proven influential, as different models applied to the same dataset can yield
111 distinct results (Araújo & New, 2007; Pearson et al., 2006, Marmion et al., 2009). This inter-
112 model variability has prompted the use of ensemble modelling techniques, also called
113 consensus modelling, which involves fitting multiple independent algorithms on the same
114 input data and then aggregating the individual models' outputs to produce a final prediction,
115 reducing the risk of overfitting and extrapolation issues (Marmion et al., 2009). While simple
116 aggregation methods like averages and weighted averages have been traditionally used
117 (Marmion et al., 2009; Hao et al., 2019), more advanced ensemble techniques, such as
118 stacking or stacked generalisation (Wolpert, 1992), have recently demonstrated superior
119 performance (Bonannella et al., 2022; 2023). In stacked ensemble modelling, multiple base
120 models' predictions serve as inputs for a meta-learner, which learns from these predictions
121 and generates the ultimate prediction by combining information from all the base models.

122 Motivated by these considerations, our study introduces a spatio-temporal stacked
123 model to infer the abundance of *Aedes albopictus*' eggs in Southern Europe from 2010 to
124 2022. The "Asian tiger mosquito" (*Aedes (Stegomyia) albopictus* (Skuse, 1895)) serves as a
125 compelling case study because it is an invasive alien species with a rapidly expanding range
126 (Roche et al., 2015; Ibáñez-Justicia, 2020) and it has medical interest due to its role of
127 vector in several outbreaks of vector-borne diseases occurred in Mediterranean Europe
128 during the last two decades (Rezza et al., 2007; Venturi et al., 2017; Brady et al., 2019;
129 Barzon et al., 2021).

130 Local public health authorities have established surveillance and monitoring
131 initiatives to gain deeper insights into the distribution, abundance and seasonality of this

132 vector, facilitating the development of proactive strategies for population and disease control.
133 Consequently, the collection of these monitoring data is necessary for the implementation of
134 passive surveillance systems, as outlined by Caputo and Manica (2020). These systems
135 encompass modelling techniques that can reliably calculate and predict vector abundance
136 and seasonal patterns, offering invaluable assistance to local public health agencies. While
137 correlative models have been widely used to infer the geographic distribution of *Ae.*
138 *albopictus* in support of surveillance and monitoring activities (Lippi et al., 2023), to the best
139 of our knowledge this is the first application of a stacked spatio-temporal model on this
140 species. This study not only contributes to the first application of a stacked spatio-temporal
141 model to *Ae. albopictus* but also offers specific results to support public health authorities in
142 planning vector control activities and assessing disease risk. The model enables the
143 inference of seasonal abundance even in areas lacking active surveillance, providing crucial
144 support for resource allocation in monitoring and surveillance efforts. Beyond its immediate
145 application, our work presents a versatile modelling framework adaptable to infer the spatio-
146 temporal abundance of various species, extending its relevance beyond the specific case of
147 *Ae. albopictus*.

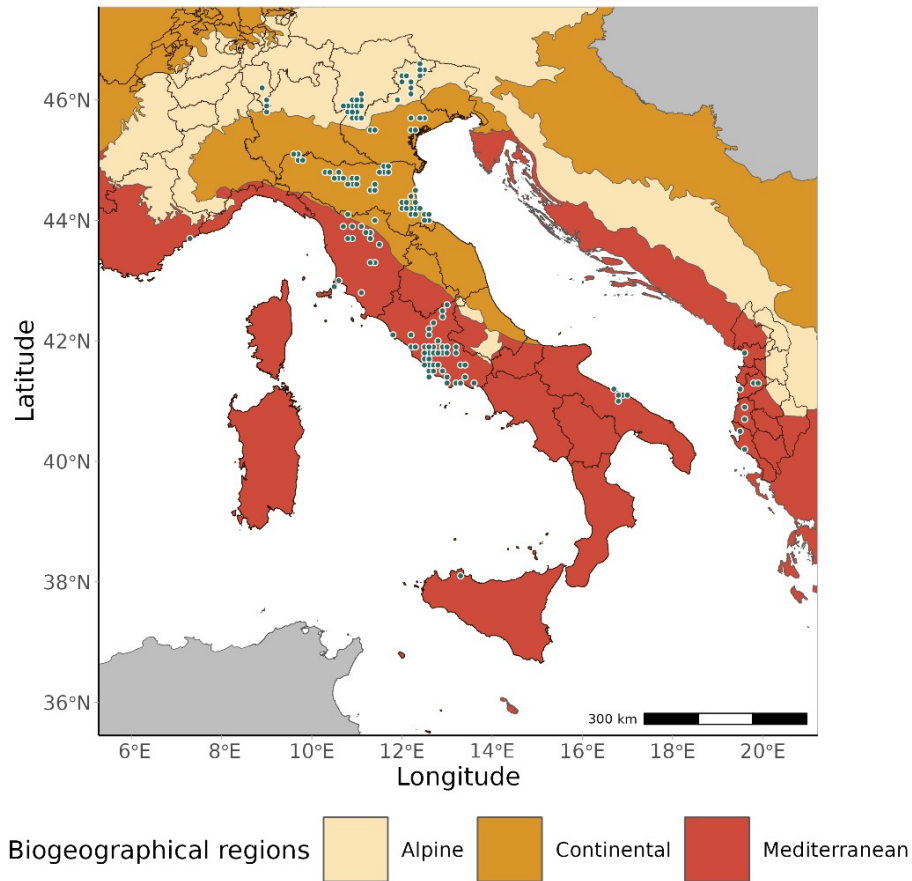
148 2. Methods

149 2.1 Biological observations and area of interest

150 We used *Ae. albopictus*' egg counts obtained from monitoring activities conducted
151 with ovitraps as the response variable in our models. Ovitrap are cheap and efficient
152 monitoring tools consisting of a dark container filled with water and a substrate where
153 container-breeding mosquitoes can lay their eggs. The stick is collected on a weekly or
154 biweekly basis, depending on the local protocol adopted by the stakeholders, and the
155 number of eggs laid on the stick counted.

156 We collected ovitraps observations from four European countries (Albania, France,
157 Italy, and Switzerland) that had active monitoring and surveillance programs of *Ae.*
158 *albopictus* utilising ovitraps between 2010 and 2022 (see Da Re et al. 2023b for a detailed
159 description of the sampling protocols and the observations pre-processing). We chose the
160 week as the fundamental temporal unit of our study; therefore, if the monitoring period
161 extended beyond one week, the observed egg counts were distributed randomly over the
162 period of trap activity using a binomial draw with a probability equal to $1/n$ weeks of
163 activation. This means that if a trap was active for 2 weeks and collected 500 eggs, the
164 observed 500 eggs would be randomly assigned to each week with a probability $p=1/2$,
165 resulting in, e.g. 256 eggs collected during the 1st week and 244 collected during the
166 second. In addition, we aggregated the ovitraps by the median using a grid of 9x9 km spatial
167 resolution (i.e., the native spatial resolution of the ERA5Land climatic datasets; Muñoz-
168 Sabater et al., 2021) to reduce the inherent variability related to the microclimatic conditions
169 to whom the single ovitraps are exposed, and mild the artefacts produced by different
170 sampling strategies and size of the ovitraps.

171 The collected ovitraps observations are located in a geographical extent spanning
172 from 6° to 21° E and from 36° to 47° N (Fig. 1). According to Cervellini et al. (2020), this area
173 is characterised by three main biogeographical regions, namely Alpine, Continental, and
174 Mediterranean (Fig. 1). Since the location of the ovitraps well represents these three
175 biogeographical regions, we decided to limit the geographical area of extrapolation of the
176 model to the abovementioned geographical extent and these biogeographical regions only.

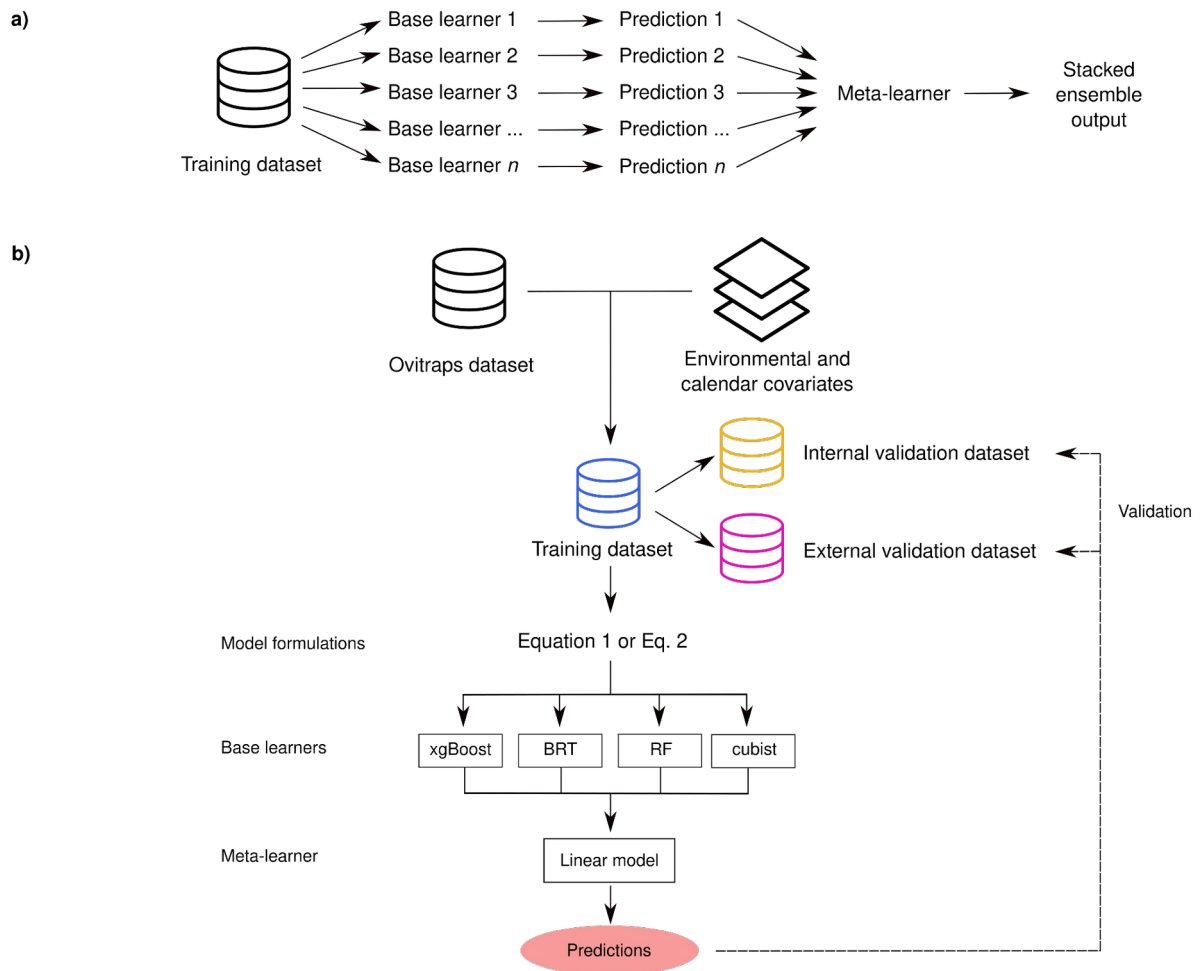


178 **Fig. 1** Biogeographical regions of Europe according to Cervellini et al., (2020) and the
 179 location (green dots) of the aggregated egg observations at 9x9 km spatial resolution. The
 180 black lines represent the borders of the administrative areas of the countries of interest at
 181 the NUTS2 level.

182

183 2.2 Modelling

184 Stacked generalisation is a technique that combines predictions from multiple
 185 individual models, known as base learners or base models, to make a final prediction
 186 (Wolpert, 1992; Boehmke and Greenwell, 2019; Bonannella et al., 2022). In stacked
 187 generalisation, the outputs of individual base learners serve as inputs to a meta-learner,
 188 which is another model that learns from the predictions of the individual models. The meta-
 189 learner then generates the final prediction by combining and synthesising the information
 190 from the individual models (Fig. 2a). Stacking has the potential to improve the accuracy and
 191 robustness of ecological models by leveraging the strengths of different models and
 192 effectively capturing complex relationships in the data (Bonannella et al., 2022). However, it
 193 is important to remark that while stacking can reduce model variance and improve
 194 predictions, it comes with trade-offs as it increases model complexity, reduces
 195 interpretability, and augments the computational time compared to individual models (Zhou,
 196 2012).



197
198

199 Fig 2. a) a conceptual representation of the stacking approach; b) framework of the
200 modelling approach presented in the study.

201 2.2.1 Model formulation

202 As with all correlative models, stacked models require providing each base learner
203 with a response variable and a set of covariates. We used as a response variable the
204 spatially aggregated weekly median egg observations described in section 2.1. As
205 covariates, we selected three main environmental drivers that significantly influence the
206 behaviour and development of mosquitoes, namely temperature, photoperiod (i.e., duration
207 of daylight in 24 hours) and precipitation (Toma et al., 2003; Becker et al., 2010; Roiz et al.,
208 2010, 2011; Marini et al. 2020; Romiti et al., 2021; Carrieri et al., 2023; see SM1.1 for a
209 detailed description of the covariates used, their ecological significance, and the
210 preprocessing operations). For each of these three covariates, we considered also their
211 lagged values, since the mosquito life cycle can take several days or weeks to complete
212 (Becker et al., 2010; Roiz et al., 2010). The lagged temperatures and photoperiod were
213 calculated as the median value between the observations recorded in the current week (i),
214 the previous week (i-1), and the week before that (i-2), whilst the lagged precipitation was
215 computed as the cumulative weekly value between the precipitation recorded in the current
216 week (i), the previous week (i-1), and the week before that (i-2).

217 In addition to the environmental covariates, which we include as distributed lags, we
 218 considered seasonal and cyclical components. Specifically, we used the Fourier series, with
 219 sine and cosine harmonic waves, to accommodate the yearly pattern and shorter-term
 220 seasonality. For these calendar effects the Fourier terms offer a more parsimonious
 221 representation than dummy variables, in particular when the frequency of the data is large
 222 (see Hyndman and Athanasopoulos 2021, Ch. 7 Sect. 4). We selected four relevant
 223 harmonic: one pair of harmonics is used for describing the yearly evolution, whereas another
 224 pair of harmonics is needed to capture some seasonal patterns. The four trigonometric
 225 waves were added to the other environmental predictors and provided a significant
 226 contribution to describing the cyclic patterns and fluctuations in the median weekly number
 227 of eggs.

228

229 Based on the results of the explorative modelling (SM1.2), we designed two different
 230 but complementary models. The regression model infers the number of eggs as a function of
 231 temperature, photoperiod, and precipitation, all lagged by -2 and -3 weeks, and the four
 232 Fourier's harmonics (Eq. 1).

233

234 (Eq. 1) Regression model: $Egg\ count \sim Temperature.lag2 + Temperature.lag3 +$
 235 $Photoperiod.lag2 + Photoperiod.lag3 + CumulativePrec.lag2 + CumulativePrec.lag3 +$
 236 $SineYear + CosineYear + SineSeasonal + CosineSeasonal$

237

238 The autoregressive model adds to the predictors considered in the Regression model (Eq. 1)
 239 an autoregressive component based on the number of eggs observed at week t-1 (Egg
 240 count.lag1).

241

242 (Eq. 2) Autoregressive model: $Egg\ count \sim Egg\ count.lag1 + Temperature.lag2 +$
 243 $Temperature.lag3 + Photoperiod.lag2 + Photoperiod.lag3 + CumulativePrec.lag2 +$
 244 $CumulativePrec.lag3 + SineYear + CosineYear + SineSeasonal + CosineSeasonal$

245 2.2.2 Stacked model

246 Each model formulation was applied to four individual base algorithms, namely
 247 extreme gradient boosting (xgBoost), boosted regression trees (BRT), random forest (RF)
 248 and cubist (Fig. 2b).

249 Extreme gradient boosting (xgBoost) is a powerful gradient boosting algorithm based
 250 on the concept of boosting, where weak models (typically decision trees) are sequentially
 251 trained to correct the mistakes made by the previous models (Friedman, 2001). The
 252 algorithm optimises an objective function by iteratively adding models to the ensemble,
 253 minimising the loss. xgBoost employs a gradient-based approach to improve the
 254 performance of the weak models and handle complex interactions among variables. Boosted
 255 regression trees (BRT) is a boosting algorithm that combines multiple decision trees to form
 256 an ensemble model (Elith et al., 2008). Similar to xgBoost, BRT sequentially trains decision
 257 trees, with each subsequent tree focusing on correcting the errors made by the previous
 258 trees. The algorithm optimises an objective function by iteratively adding trees, and the final
 259 prediction is a weighted sum of the predictions from all the trees. Random Forest is an
 260 ensemble learning method that constructs a collection of decision trees and combines their
 261 predictions to make accurate predictions (Breiman, 2001). Each tree in the RF is built on a
 262 randomly sampled subset of the data and a randomly selected subset of features. This

263 randomness helps to reduce overfitting and increase the diversity among the trees, and the
264 final prediction is determined by averaging or voting the predictions from all the trees in the
265 forest. Finally, cubist is a rule-based algorithm that combines decision trees with linear
266 models. It creates a set of rules by recursively partitioning the data based on the predictor
267 variables (Quinlan, 1992). Each rule corresponds to a specific region of the feature space
268 and predicts the response variable using a linear model. The algorithm iteratively builds a
269 series of decision trees and linear models, optimising an objective function that balances
270 accuracy and complexity.

271 We tuned the hyperparameters of each of the four machine-learning algorithms for
272 both model formulations (Eq. 1-2; SM2.1). Then, for each model formulation separately, we
273 combined the predictions of each tuned algorithm into the meta-learner, defined as a linear
274 regression of the egg count (response variable) and the four algorithms' predictions
275 (covariates). Both meta-learners were used to predict the abundance of *Ae. albopictus* eggs
276 over the period 2010-2022 on the training and validation datasets. The meta-learner trained
277 with the four algorithms having as model formulation Eq. 1, i.e. the regression model, was
278 also used to predict, and thus extrapolate, over the whole area of interest for the period
279 2010-2022.

280 All the analyses were performed in R 4.3 (R Core Team 2023). All the R scripts used
281 for the analysis are available at the GitHub repository <https://github.com/danddr/stackedML>.
282 The R scripts are shared with detailed comments to foster the methodology reproducibility
283 and its application to case studies and species different to invasive mosquitoes.

284

285 2.3 Model validation

286 The aggregated egg observations were partitioned into one training and two testing
287 datasets (Fig. 2b). To conduct external validation, we employed a random selection process,
288 choosing two aggregated ovitraps within each distinct NUTS2 level for every biogeographical
289 region. This selection was limited to aggregated ovitraps with a minimum of three years'
290 worth of observations, guaranteeing the presence of a robust time series for validation.
291 These observations were excluded from the training dataset allowing for an exhaustive
292 coverage of the longitudinal and latitudinal gradient of the area of interest. We excluded
293 Sicily from the external validation dataset because it hosts only one aggregated ovitrap and
294 represents the southernmost observation in the area of interest (see Fig. S3.1 for the
295 locations of the ovitraps used for the external validation). After excluding these stations, we
296 defined the training dataset as all the observations spanning from 2010 to 2021 and the
297 testing dataset as all the observations gathered in 2022. As an additional validation, we also
298 performed a 10-fold cross-validation on the training dataset by retaining, for each fold, 70%
299 of the observations to train the model. The class of models used is either regression or
300 autoregression, so the standard k-fold cross-validation can be implemented, as suggested
301 by Hyndman and Athanasopoulos (2021, Ch 5. Sect. 10). To estimate the model's predictive
302 error we estimated, for each station and validation dataset, the root mean squared error
303 (RMSE) and the mean absolute error (MAE).

304 2.4 Deriving pseudo-phenological indexes: introducing the 305 period-over-threshold

306 In addition to utilising the stacked model for predicting the average number of eggs
307 for each week within a given year across the area of interest, we also aimed to derive
308 estimates about the predicted seasonality of *Ae. albopictus*. Different approaches have been
309 proposed to compute seasonal indexes of mosquitoes like onset (i.e. beginning of the
310 season), peak, and offset (i.e., end of the season; Rosà et al., 2014, Romiti et al., 2022).
311 However, these approaches assume a repeated and even sampling of the species of
312 interest, which, unfortunately, is not the case across the sampling locations of our dataset.
313 Therefore, here we propose and define a pseudo-seasonal index that we call the period-
314 over-threshold (POT).

315 The POT represents the period in which the variable of interest, i.e. the average
316 number of eggs, is above a certain threshold. The POT might be of interest not only for
317 spatial epidemiological applications but also for alien species monitoring or biological
318 conservation, i.e. by identifying the areas and the period in which a given population is below
319 or above a certain threshold and therefore requires local interventions. Here, we define the
320 POT as the number of weeks in which the weekly average number of eggs is equal to or
321 higher than 55 eggs, the spatially and weekly aggregated average median number of eggs
322 (excluding zeros) observed over the whole area of interest during the period 2010-2022. We
323 acknowledge that the POT, as defined here, is a heuristic approach, and therefore we
324 performed a sensitivity analysis varying the threshold to 20 and 125, defined by the average
325 interquartile range (IQR) of the observed distribution.

326 Finally, we investigated if the observed and predicted POT have varied in time and
327 space among the different biogeographical regions over the 2010-2022 period. We tested
328 whether the length of the observed and estimated POT is affected by the year (quantitative)
329 and the biogeographical regions (qualitative: Alpine/Continental/Mediterranean) and their
330 interaction, using Generalised Linear Mixed Models (GLMMs) with Poisson error distribution
331 and log link function, considering the ID of the aggregated ovitraps as a random factor.

332 3. Results

333 3.1 Ovitrap dataset descriptive statistics

334 We collected observations from 2620 ovttraps in four European countries (Albania, France,
335 Italy and Switzerland), resulting in 149 aggregated ovttraps stations after the aggregation at
336 9x9 km spatial resolution. Overall, 30 aggregated ovttraps were located in the Alpine
337 biogeographical region, while 48 and 71 were located in the Continental and Mediterranean
338 biogeographical regions, respectively. Most of the ovttraps were active during the period
339 2020-2022, with only a few stations that were monitored for more than three seasons (Da Re
340 et al. 2023b). 120 aggregate ovttraps were used to train the models, whilst 19 were retained
341 for the external validation.

342 3.2 Model outputs

343 The random forest algorithm showed the highest regression coefficient in the regression
344 stacked model and so resulted as the most important algorithm (Tab. S2.2), while the most
345 important environmental predictors were the 3-week-lagged temperature and photoperiod
346 (Fig. S2.3A). On the other hand, cubist was the most important algorithm for the stacked
347 autoregressive model, with the 1-week-lagged value of observed eggs being the most
348 important predictor (Fig. S.2.3B).

349 Both stacked models were able to capture the seasonal and interannual variability of
350 the ovttraps time series in the training dataset and both validation datasets (Fig. 3, Fig.
351 S3.2). A detailed representation of the external validations for both models, broken down at
352 the location level, is available in SM3 in Fig. S3.3-S3.4 for the regression and autoregressive
353 models respectively. The predicted values for both the internal and external validation
354 matched the observation patterns in the three biogeographical regions, with the
355 autoregressive model showing, in general, a closer association with the observations. The
356 autoregressive model showed overall a higher R^2 and lower RMSE and MAE compared to
357 the regression model in the training and both validation datasets (Tab. 1; Fig. S3.5).

358

359 **Tab. 1** Stacked model validation metrics from the 10-fold cross-validation made on the
360 training dataset.

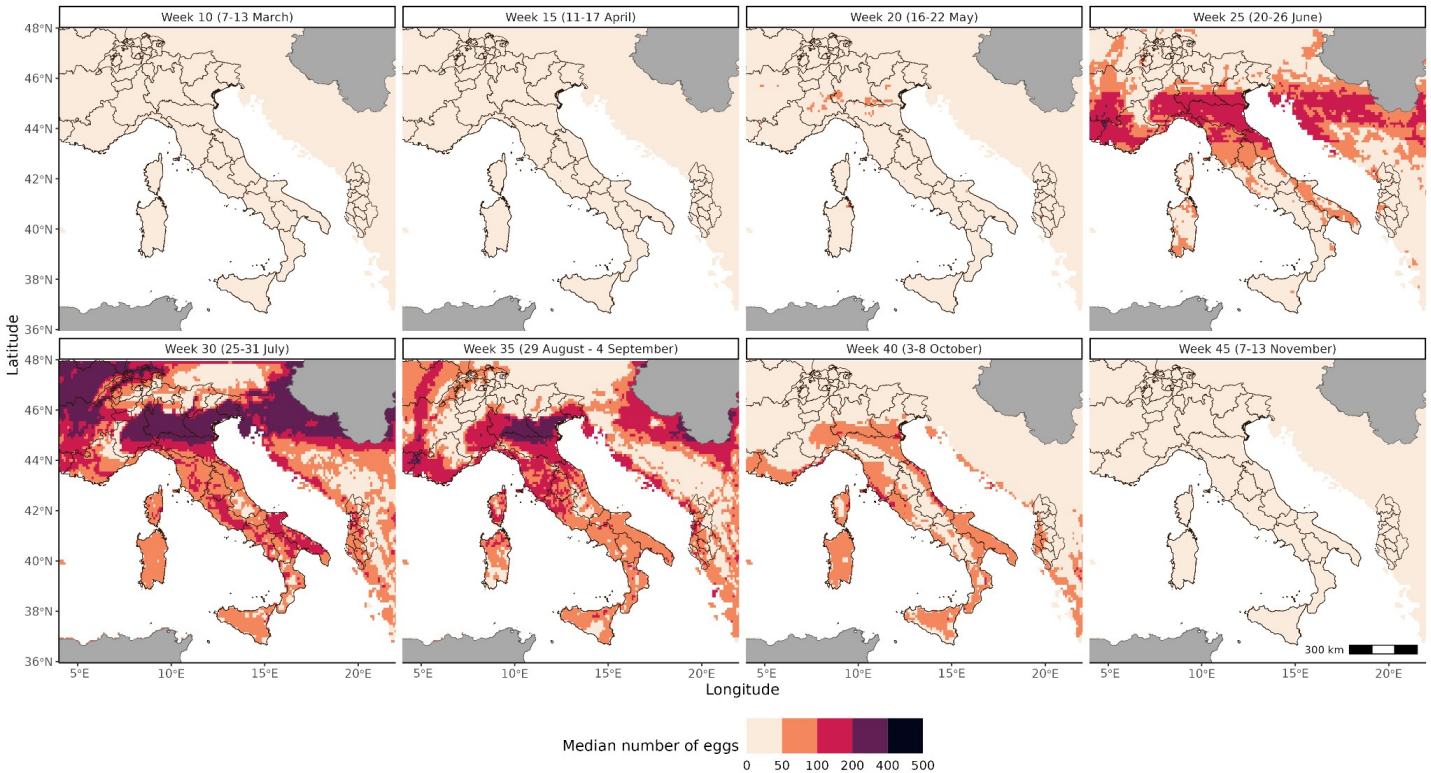
Model	R^2	Residual standard error	10-fold CV RMSE	10-fold CV MAE
<i>Regression</i>	0.63	55.55	50.37	24.44
<i>Autoregressive</i>	0.85	35.38	34.39	12.66

361

362



364 **Fig. 3** Median and interquartile range of the number of eggs observed (grey lines) and
 365 predicted by the regression model in both the internal and external validation. Both the
 366 observed and predicted values were aggregated over the three biogeographical regions to
 367 allow an easier representation.



369 **Fig. 4.** Median number of eggs predicted weekly by the regression model in the area of
370 interest for the year 2022. The black lines represent the borders of the administrative areas
371 of the countries of interest at the NUTS2 level. The grey areas are outside the area of
372 interest.

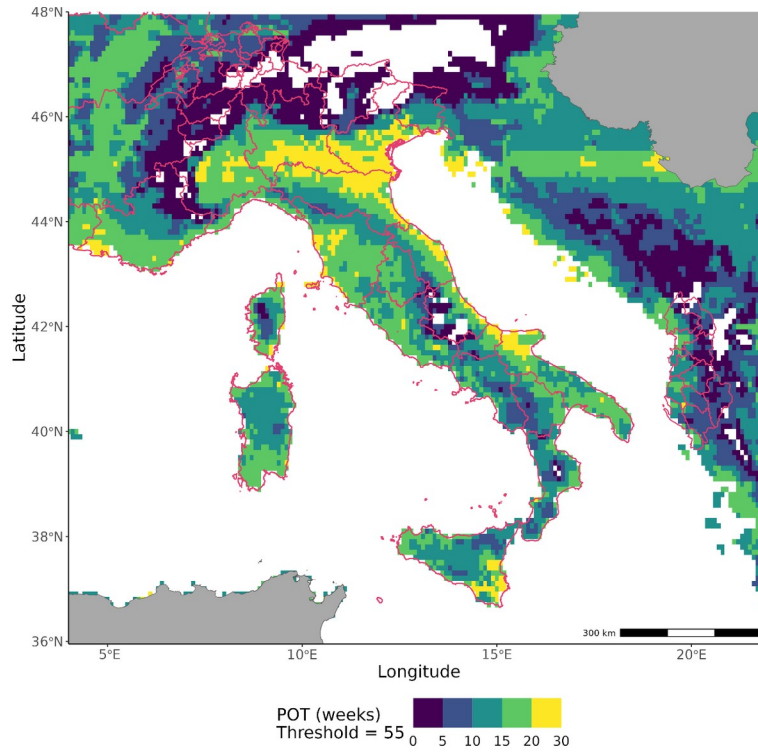
373 3.3 Spatial predictions

374 The spatio-temporal predictions of the stacked regression model for the year 2022
375 show seasonal and latitudinal variation in the area of interest (Fig. 4). Generally, we observe
376 an average number of eggs higher than 50 in the entire study area from week 20 (mid-May)
377 onwards. The peak of the season is estimated on week 30 (end of July), especially in the Po
378 and Rhone valleys, as well as in the coastal areas of the Adriatic, Ionian and Tyrrhenian
379 seas. The predicted average number of eggs decreases after week 35 (end of August). Still,
380 it follows a latitudinal and geographical shift, with the Southernmost and coastal areas
381 showing predicted values of eggs higher than 100 still in week 40 (beginning of October),
382 decreasing below fifty only after week 45 (November) onwards.

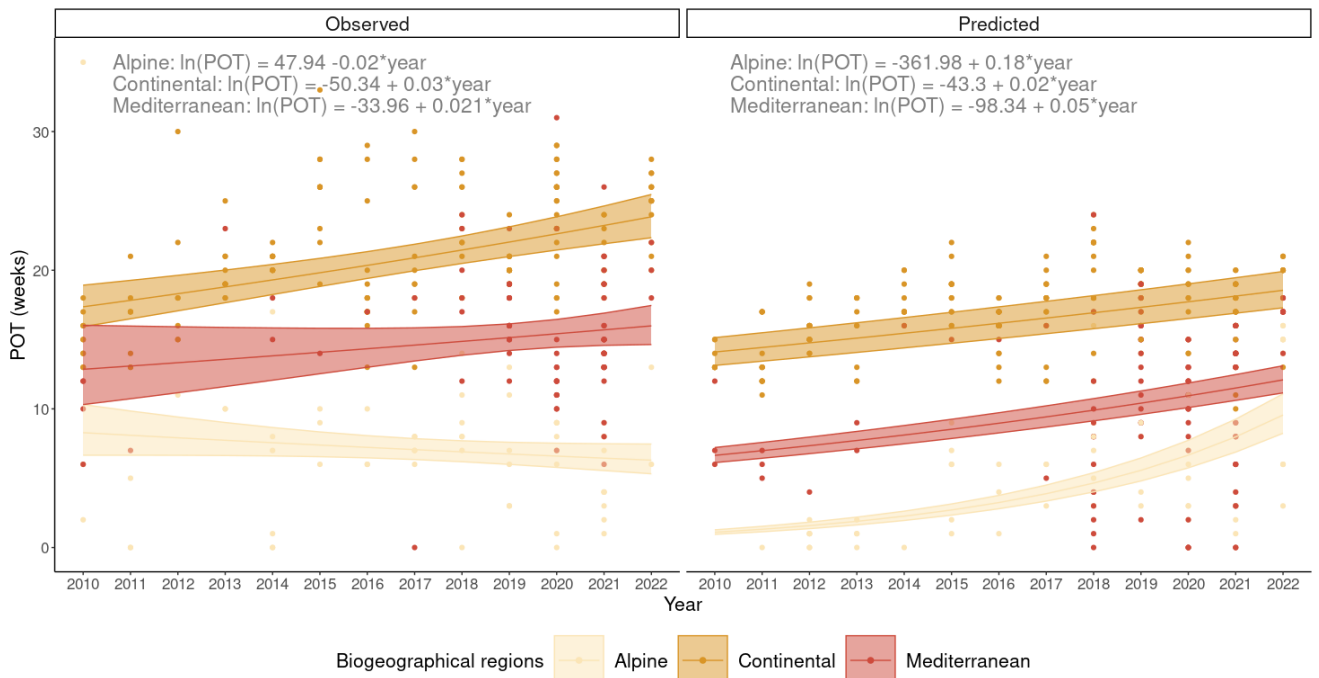
383 3.4 Period-over-threshold

384 On average, the observed POT spans 7 (6-9 IQR) weeks for the Alpine
385 biogeographical region, 20 (19-22 IQR) and 15 (14-16 IQR) weeks for the Continental and
386 Mediterranean biogeographical regions, respectively. The predicted POT shows generally a
387 shorter length, with 4 (3-5 IQR) weeks for the Alpine biogeographical region, and 17 (16-18
388 IQR) and 11 (9-12 IQR) weeks for the Continental and Mediterranean biogeographical
389 regions respectively. The spatial representation of the POT for the year 2022 (Fig. 5) shows
390 a longer length of the POT in the Po Valley and coastal zones of the area of interest (POT >
391 20 weeks). Mountainous and foothills areas show, on average, short (POT \leq 5) or absent
392 POT.

393 The Poisson GLMMs investigating the effect of the interaction between the year and
394 the biogeographical regions on the POT show significant effects for all the explanatory
395 variables and their interactions, except for the Alpine biogeographical region in the Observed
396 (Tab. S3.7). The predicted values of the models trained on the observed and estimated POT
397 showed a positive increase, independent from the reference year, for all the biogeographical
398 regions but the Alpine in the observed dataset over the period 2010-2022 (Fig. 6).



399
 400 **Fig. 5.** Spatial representation of the critical period-over-threshold (POT) for the year 2022 in
 401 the area of interest. White pixels are characterised by an average median weekly number of
 402 eggs always lower than 55. The pink lines represent the borders of the administrative areas
 403 of the countries of interest at the NUTS2 level.
 404
 405



406
 407 **Fig. 6.** Modelled relationships between the Period-over-threshold and the interaction
 408 between the year and biogeographical regions using a Poisson GLMM.
 409

410 4. Discussion

411 Ensemble modelling is a popular technique to mitigate the artefacts or errors that
412 may arise from individual algorithm predictions. Among the different ensemble techniques
413 available, stacking has recently risen as one of the approaches leading to a more robust and
414 accurate final prediction (Bonannella et al., 2022; 2023). In this study, we proposed a
415 reproducible application of a stacked model to infer the spatio-temporal abundance of a
416 species of interest, the Tiger mosquito *Ae. albopictus*. We stress that our approach can be
417 replicated and applied to different species, not only those of medical interest if longitudinal
418 observations on their abundance and phenology are available. The application of a stacked
419 model on both regression and autoregressive model formulations resulted in reliable
420 estimates of mosquito egg abundance. Such results can contribute to supporting local public
421 health authorities' efforts in mosquito management and control: the regression model in
422 particular allowed us to rapidly infer the weekly egg abundance in areas not covered by
423 monitoring activities. This is extremely important to support local public health authorities to
424 better allocate monitoring and surveillance resources and to simulate scenarios for the next
425 mosquito season under different climatic conditions.

426

427 4.1 Predictive accuracy of the models

428 The performance metrics of the regression and autoregressive models indicated a
429 consistently strong predictive accuracy throughout the entire time series. Furthermore, the
430 values of RMSE and MAE displayed similarities between the internal and external validation
431 datasets. The autoregressive model showed generally higher predictive performance than
432 the regression model, having the lagged number of eggs observed as the most important
433 predictive variable. This was not unexpected, since the preliminary exploratory analysis (SM
434 1.2), made with genuine regression models, displayed strong empirical autocorrelation, of
435 order one, in the residuals. However, the high predictive accuracy of the autoregressive
436 model has the drawback of not being able to spatially extrapolate its predictions outside the
437 training dataset. Whilst this can be seen as a limitation, it offers the opportunity of having
438 accurate estimates and forecasts in specific locations, allowing the model to be informed
439 with local and high-quality environmental information, using e.g. weather station
440 observations. On the contrary, the regression model allowed us to spatially extrapolate the
441 predictions in areas that were not previously sampled. The median number of eggs predicted
442 over the study area for the year 2022 matches the expected seasonal dynamic of the
443 species. Though egg-laying activity might occur in March and April, it increases around week
444 20 (mid-May) and ends in early October following elevational and latitudinal gradients
445 (Romiti et al., 2022; Carrieri et al., 2023; Lencioni et al., 2023). In the alpine areas, our
446 spatial estimates resembled those obtained using different modelling techniques and training
447 datasets (e.g. Ravasi et al., 2022). Previous dynamical distribution modelling approach
448 forecasting *Ae. albopictus* eggs abundance at high spatial (0.01 latitudinal and longitudinal
449 degrees) and temporal (weekly) resolution over ten Balkan countries projected annual peaks
450 in egg abundance between the summer months of August and September i.e. approximately
451 from weeks 32 to 38 (Tisseuil et al., 2018). The field investigation in Albania in 2023 has
452 shown the peak of the season in July (weeks 28-29-30) and another peak at the end of
453 August and beginning of September (weeks 35-36; personal communication of E. Velo). For
454 the coastal areas of the Tyrrhenian Sea, the spatio-temporal prediction of the stacked

455 regression model confirms the results of previous studies carried out in central Italy, where
 456 the peak of activity and the end of the season is expected at the end of August and
 457 November, respectively (Fig. 4; Romiti et al., 2021; 2022). Interestingly, these estimates
 458 based on ovitrap data (i.e. collection of eggs) comply with independent estimates obtained
 459 from data acquired collecting a different life stage of the mosquito (i.e., host-seeking
 460 females) at the two opposite ends of Italy (Trentino and Sicily) that identified the beginning of
 461 the season in mid-June and mid-March and the peak of the season in early August and
 462 August-September, respectively (Guzzetta et al., 2016; Torina et al., 2023).

463

464 4.2 Period-over-threshold

465 The pseudo-phenological index POT computed for *Ae. albopictus* during the year
 466 2022 also showed latitudinal and elevational gradients, with the Po Valley and coastal areas
 467 having generally longer POT than mountainous areas. In the coastal areas of the Tyrrhenian
 468 Sea, the estimated POT is between 15 and 20, decreasing to 5 weeks in low mountain areas
 469 and to zero in high mountain peaks, similar to what was described in previous studies
 470 (Romiti et al., 2021; 2022). The spatial pattern depicted in Fig. 5 resembles those
 471 representing the estimates *Ae. albopictus* seasonal length presented by Petric et al. (2021).
 472 However, the estimates of Petric et al. (2021), based on multiple conditional statements of
 473 temperature and photoperiod, show a generally longer period of activity of the species
 474 compared to the estimated POT. This is not unexpected, because the two outputs are
 475 intrinsically different: the POT measures the length of the period over a user-defined
 476 threshold, whilst Petric et al. (2021) have estimated the length of the period of activity of the
 477 mosquito considering the environmental conditions triggering eggs hatching, which in
 478 Mediterranean areas can begin in early March though at low density (Petric et al., 2021).

479 In both the Continental and Mediterranean biogeographical regions, both observed
 480 and estimated POT durations have been increasing by approximately one week every year.
 481 This trend suggests a potential direct impact of global warming on the abundance of this
 482 species, as discussed in previous studies (Kramer et al., 2021; Oliveira et al., 2021; Del
 483 Lesto et al., 2022; Romiti et al., 2022; Lühsen et al., 2023). However, it is also essential to
 484 consider that the prolonged POT duration might be influenced by other factors, such as the
 485 increased monitoring efforts and the expanding range of the insect, leading to higher
 486 observed counts and longer POT periods.

487 Other threshold-based indexes have been proposed specifically for *Ae. albopictus*,
 488 but those are mostly epidemiological indexes (e.g. Carrieri et al., 2012; Aryaprema et al.,
 489 2023). We believe that the strength of the POT method lies in its broad interpretability and
 490 applicability. This approach can be employed not only in spatial epidemiology applications,
 491 as demonstrated in our case study but also in monitoring alien species or supporting
 492 biological conservation efforts. It enables the identification of locations and periods when a
 493 particular population falls below or surpasses a defined threshold, signalling the need for
 494 targeted local interventions.

495

496 4.3 Limitations and future perspectives

497 As for most ecological models, one of the main limitations of these results relies on
 498 the quantity and quality of the training dataset (Cayuela et al., 2009). First of all, egg
 499 observations were pooled from ovitraps having different volumes, shapes, oviposition
 500 substrates, liquid solutions, revisit times, etc. (Da Re et al., 2023b). This, unfortunately, is a
 501 limitation related to the different sampling and monitoring schemes employed by the different

502 institutions (Da Re et al., 2023b). Despite the preprocessing operation on the observations
503 collected by the ovitraps, some of these sources of variability have likely influenced our
504 results and therefore should be taken into account while interpreting the results. Therefore,
505 we want to highlight the importance of carrying out reproducible and comparable sampling
506 schemes following the most updated standards for ovitraps monitoring, as those presented
507 as the outcome of the AIM-COST cost action by Miranda et al. (2022).

508 Our dataset is also spatially biased because most of the observations are spatially
509 clustered in north-central Italy, especially in the Emilia-Romagna region, where one of the
510 most consistent and long-lasting surveillance programs has been carried out since 2010.
511 The observations coming from this region had likely the highest quality, having been
512 sampled continuously every two weeks from 2010 onwards. Spatial clustering is known to
513 bias the models' estimates and predictions (Sillero and Barbosa, 2020) and therefore has
514 likely produced sub-optimal predictions in the southern part of the area of interest. This
515 detrimental aspect of our outputs can only be resolved by increasing the sampling effort in
516 the southern part of the study area.

517 Another potential source of variability in the training dataset is the effect of vector
518 control practices affecting the abundance of collected eggs. Pest control agencies act to limit
519 the abundance of the species and reduce the nuisance the bites are causing to the
520 population (Ravasi et al., 2021). Unfortunately, this is an effect that we cannot control, as we
521 do not have access to the location and period of each pest containment treatment carried
522 out in the area and period of interest.

523 Despite these limitations, the proposed framework seems feasible to be implemented
524 to produce both local and continental scale predictions and forecasts, contributing to
525 supporting the stakeholders in their effort against *Ae. albopictus*. Using e.g. regional
526 circulation models and/or weather generators, the methodology presented here can be used
527 to produce estimates for the next seasons under different climatic scenarios. Interestingly,
528 the presented methodology can be implemented and corrected during the season by
529 including the results of the monitoring activities in the training dataset. The estimates of
530 these models can also be compared to estimates produced by other correlative models (e.g.
531 Georgiades et al 2023), or mechanistic models such as *albopictus* (Erguler et al., 2016),
532 and *dynamAedes* (Da Re et al., 2022), producing a plethora of models' estimates
533 accounting for different aspects of the biological system studied.

534 By employing the results of our modelling approach, public health authorities can
535 make informed decisions regarding the implementation of control measures, allocation of
536 resources, and targeted interventions to mitigate the risks posed by invasive mosquitoes and
537 safeguard human and animal health. The latter aspect has gained particular interest during
538 the past two decades when the impact of invasive species on public health has become
539 more evident (e.g., Zink et al., 2012; Schaffner et al., 2020). Apart from the public health
540 aspect, we believe our work has a broader scope, providing a tool that can be adapted to
541 infer the spatio-temporal abundance and seasonality of different species of interest.

542 **5. References**

543

544 Araújo M.B., New M. 2007. Ensemble forecasting of species distributions. *Trends in Ecology &*
545 *Evolution* 22(1):42-47

546

547 Aryaprema, V. S., Steck, M. R., Peper, S. T., Xue, R. D., & Qualls, W. A. (2023). A systematic review
548 of published literature on mosquito control action thresholds across the world. *PLOS Neglected*
549 *Tropical Diseases*, 17(3), e0011173.

550

551 Barzon, L., Gobbi, F., Capelli, G., Montarsi, F., Martini, S., Riccetti, S., ... & Lazzarini, L. (2021).
552 Autochthonous dengue outbreak in Italy 2020: clinical, virological and entomological findings. *Journal*
553 *of travel medicine*, 28(8), taab130.

554

555 Bazzichetto, M., Lenoir, J., Da Re, D., Tordoni, E., Rocchini, D., Malavasi, M., ... & Sperandii, M. G.
556 (2023). Sampling strategy matters to accurately estimate response curves' parameters in species
557 distribution models. *Global Ecology and Biogeography*, 32, 1717–1729

558

559 Becker, N., Petric, D., Zgomba, M., Boase, C., Madon, M., Dahl, C., & Kaiser, A. (2010). *Mosquitoes*
560 *and their control*. Springer Science & Business Media.

561

562 Boehmke, B., & Greenwell, B. M. (2019). Chap. 15: Stacked models. In: *Hands-on machine learning*
563 *with R*. CRC press.

564

565 Bonannella, C., Hengl, T., Heisig, J., Parente, L., Wright, M. N., Herold, M., de Bruin, S. (2022).
566 Forest tree species distribution for Europe 2000–2020: mapping potential and realized distributions
567 using spatiotemporal machine learning. *PeerJ* 10:e13728 <https://doi.org/10.7717/peerj.13728>

568

569 Bonannella, C., Hengl, T., Parente, L., de Bruin, S. (2023). Biomes of the world under climate change
570 scenarios: increasing aridity and higher temperatures lead to significant shifts in natural vegetation.
571 *PeerJ* 11:e15593 <https://doi.org/10.7717/peerj.15593>

572

573 Brady, O. J., & Hay, S. I. (2019). The first local cases of Zika virus in Europe. *The Lancet*,
574 394(10213), 1991-1992.

575

576 Breiman, L. (2001). Random forests. *Machine learning*, 45, 5-32.

577

578 Burkett-Cadena, N. D., McClure, C. J., Ligon, R. A., Graham, S. P., Guyer, C., Hill, G. E., ... &
579 Unnasch, T. R. (2011). Host reproductive phenology drives seasonal patterns of host use in
580 mosquitoes. *PLOS one*, 6(3), e17681.

581

582 Carrieri, M., Albieri, A., Angelini, P., Soracase, M., Dottori, M., Antolini, G., & Bellini, R. (2023). Effects
583 of the Weather on the Seasonal Population Trend of *Aedes albopictus* (Diptera: Culicidae) in Northern
584 Italy. *Insects*. 2023; 14(11):879. <https://doi.org/10.3390/insects14110879>

585

586 Carrieri, M., Angelini, P., Venturelli, C., Maccagnani, B., & Bellini, R. (2012). *Aedes albopictus*
587 (Diptera: Culicidae) population size survey in the 2007 Chikungunya outbreak area in Italy. II:
588 estimating epidemic thresholds. *Journal of Medical Entomology*, 49(2), 388-399.

589

590 Cayuela, L., Golicher, D. J., Newton, A. C., Kolb, M., De Albuquerque, F. S., Arets, E. J. M. M.,
591 Alkemade, J. R. M. & Pérez, A. M. (2009). Species distribution modeling in the tropics: problems,

- 592 potentialities, and the role of biological data for effective species conservation.
 593 *Tropical Conservation Science*, 2(3), 319-352.
 594
- 595 Caputo, B., & Manica, M. (2020). Mosquito surveillance and disease outbreak risk models to inform
 596 mosquito-control operations in Europe. *Current opinion in insect science*, 39, 101-108.
 597
- 598 Cervellini, M., Zannini, P., Di Musciano, M., Fattorini, S., Jiménez-Alfaro, B., Rocchini, D., ... &
 599 Chiarucci, A. (2020). A grid-based map for the Biogeographical Regions of Europe. *Biodiversity Data*
 600 *Journal*, 8.
 601
- 602 Da Re, D., Tordoni, E., Lenoir, J., Vanwambeke, S. O., Rocchini, D., Bazzichetto, M., & SoilTemp
 603 Consortium. (2023a). USE it: uniformly sampling pseudo-absences within the environmental space for
 604 applications in habitat suitability models. *Methods in Ecology and Evolution*, 14, 2873–2887.
 605 <https://doi.org/10.1111/2041-210X.14209>
 606
- 607 Da Re, D., et al. (2023b). VectAbundance: a spatio-temporal database of vector observations.
 608 Preprint available on EcoEvoRxiv. <https://doi.org/10.32942/>.
 609
- 610 Da Re, D., Van Bortel, W., Reuss, F., Müller, R., Boyer, S., Montarsi, F., ... & Marcantonio, M. (2022).
 611 dynamAedes: a unified modelling framework for invasive *Aedes* mosquitoes. *Parasites & vectors*,
 612 15(1), 1-18.
 613
- 614 Del Lesto, I., De Liberato, C., Casini, R., Magliano, A., Ermenegildi, A., & Romiti, F. (2022). Is Asian
 615 tiger mosquito (*Aedes albopictus*) going to become homodynamic in Southern Europe in the next
 616 decades due to climate change?. *Royal Society Open Science*, 9(12), 220967.
 617
- 618 Edwards, C. B., & Crone, E. E. (2021). Estimating abundance and phenology from transect count data
 619 with GLMs. *Oikos*, 130(8), 1335-1345
 620
- 621 Elith, J., Leathwick, J. R., & Hastie, T. (2008). A working guide to boosted regression trees. *Journal of*
 622 *animal ecology*, 77(4), 802-813.
 623
- 624 Ettinger, A. K., Chamberlain, C. J., & Wolkovich, E. M. (2022). The increasing relevance of phenology
 625 to conservation. *Nature Climate Change*, 12(4), 305-307.
 626
- 627 Fand, B. B., Choudhary, J. S., Kumar, M., & Bal, S. K. (2014). Phenology modelling and GIS
 628 applications in pest management: A tool for studying and understanding insect-pest dynamics in the
 629 context of global climate change. *Approaches to Plant Stress and their Management*, 107-124.
 630
- 631 Fourcade, Y. (2021). Fine-tuning niche models matters in invasion ecology. A lesson from the land
 632 planarian *Obama nungara*. *Ecological Modelling*, 457, 109686.
 633
- 634 Friedman, J. H. (2001). Greedy function approximation: a gradient boosting machine. *Annals*
 635 *of Statistics*, pp. 1189–1232.
 636
- 637 Georgiades, P., Proestos, Y., Lelieveld, J., & Erguler, K. (2023). Machine Learning Modeling of *Aedes*
 638 *albopictus* Habitat Suitability in the 21st Century. *Insects*, 14(5), 447.
 639
- 640 Guisan, A., Thuiller, W., & Zimmermann, N. E. (2017). *Habitat suitability and distribution models: with*
 641 *applications in R*. Cambridge University Press.
 642

- 643 Guzzetta, G., Montarsi, F., Baldacchino, F. A., Metz, M., Capelli, G., Rizzoli, A., ... & Merler, S. (2016).
 644 Potential risk of dengue and chikungunya outbreaks in northern Italy based on a population model of
 645 *Aedes albopictus* (Diptera: Culicidae). *PLoS neglected tropical diseases*, 10(6), e0004762.
 646
- 647 Hao, T., Elith, J., Guillera-Arroita, G., Lahoz-Monfort, J.J. (2019). A review of evidence about use and
 648 performance of species distribution modelling ensembles like BIOMOD. *Diversity and Distributions*
 649 25(5):839-852
 650
- 651 Hyndman, R.J., & Athanasopoulos, G. (2021) *Forecasting: principles and practice*, 3rd edition,
 652 OTexts: Melbourne, Australia. OTexts.com/fpp3. Accessed on 17 October 2023.
 653 Hortal, J., Jiménez-Valverde, A., Gómez, J. F., Lobo, J. M., & Baselga, A. (2008). Historical bias in
 654 biodiversity inventories affects the observed environmental niche of the species. *Oikos*, 117(6), 847-
 655 858.
 656
- 657 Ibáñez-Justicia, A. (2020). Pathways for introduction and dispersal of invasive *Aedes* mosquito
 658 species in Europe: a review. *Journal of the European Mosquito Control Association*, 38(1-10).
 659
- 660 Kramer, I. M., Pfeiffer, M., Steffens, O., Schneider, F., Gerger, V., Phuyal, P., ... & Müller, R. (2021).
 661 The ecophysiological plasticity of *Aedes aegypti* and *Aedes albopictus* concerning overwintering in
 662 cooler ecoregions is driven by local climate and acclimation capacity. *Science of The Total*
 663 *Environment*, 778, 146128.
- 664 Lencioni V., F. Bertola, A. Franceschini, U. Ferrarese, F. Zandonai, G. Stancher, D. Spitale (2023)
 665 Multi-year dynamics of the *Aedes albopictus* occurrence in two neighbouring cities in the Alps. *The*
 666 *European Zoological Journal*, 90(1), 101-112.
 667
- 668 Marini, G., Manica, M., Arnoldi, D., Inama, E., Rosà, R., & Rizzoli, A. (2020). Influence of temperature
 669 on the life-cycle dynamics of *Aedes albopictus* population established at temperate latitudes: A
 670 laboratory experiment. *Insects*, 11(11), 808.
 671
- 672 Marini, G., Arnoldi, D., Baldacchino, F., Capelli, G., Guzzetta, G., Merler, S., ... & Rosà, R. (2019).
 673 First report of the influence of temperature on the bionomics and population dynamics of *Aedes*
 674 *koreicus*, a new invasive alien species in Europe. *Parasites & vectors*, 12, 1-12.
 675
- 676 Marmion, M., Parviainen, M., Luoto, M., Heikkinen, R. K., & Thuiller, W. (2009). Evaluation of
 677 consensus methods in predictive species distribution modelling. *Diversity and Distributions*, 15(1), 59-
 678 69.
 679
- 680 Miranda, M. Á., Barceló, C., Arnoldi, D., Augsten, X., Bakran-Lebl, K., Balatsos, G., ... & Consortium,
 681 A. C. (2022). AIMSurg: First pan-European harmonized surveillance of *Aedes* invasive mosquito
 682 species of relevance for human vector-borne diseases. *Gigabyte*, 2022.
 683
- 684 Muñoz-Sabater J, Dutra E, Agustí-Panareda A, Albergel C, Arduini G, Balsamo G, Boussetta S,
 685 Choulga M, Harrigan S, Hersbach H, et al. ERA5-Land: A state-of-the-art global reanalysis dataset for
 686 land applications. *Earth Syst Sci Data Discuss* 2021: 1–50.
 687
- 688 Lippi, C. A., Mundis, S. J., Sippy, R., Flenniken, J. M., Chaudhary, A., Hecht, G., ... & Ryan, S. J.
 689 (2023). Trends in mosquito species distribution modeling: insights for vector surveillance and disease
 690 control. *Parasites & Vectors*, 16(1), 302.
 691
- 692 Lührsen, D. S., Zavitsanou, E., Cerecedo-Iglesias, C., Pardo-Araujo, M., Palmer, J. R., Bartumeus, F.,
 693 ... & Lowe, R. (2023). Adult *Aedes albopictus* in winter: implications for mosquito surveillance in
 694 Southern Europe. *The Lancet Planetary Health*, 7(9), e729-e731.

- 695
696 Oliveira, S., Rocha, J., Sousa, C. A., & Capinha, C. (2021). Wide and increasing suitability for *Aedes*
697 *albopictus* in Europe is congruent across distribution models. *Scientific reports*, 11(1), 9916.
698
- 699 Pearson R. G, Thuiller W., Araújo M.B., Martinez-Meyer E., Brotons L., McClean C., Miles L,
700 Segurado P, Dawson T.P., Lees D.C.. 2006. Model-based uncertainty in species range prediction.
701 *Journal of Biogeography* 33(10):1704-1711
702
- 703 Petrić, M., Ducheyne, E., Gossner, C. M., Marsboom, C., Venail, R., Hendrickx, G., & Schaffner, F.
704 (2021). Seasonality and timing of peak abundance of *Aedes albopictus* in Europe: Implications to
705 public and animal health. *Geospatial Health*, 16(1).
706
- 707 Pfab, F., Stacconi, M. V. R., Anfora, G., Grassi, A., Walton, V., & Pugliese, A. (2018). Optimized
708 timing of parasitoid release: a mathematical model for biological control of *Drosophila suzukii*.
709 *Theoretical Ecology*, 11, 489-501.
710
- 711 Quinlan, J.R., 1992, November. Learning with continuous classes. In 5th Australian joint conference
712 on artificial intelligence (Vol. 92, pp. 343-348).
713
- 714 R Core Team (2023). R: A Language and Environment for Statistical Computing. R Foundation for
715 Statistical Computing, Vienna, Austria. <https://www.R-project.org/>.
716
- 717 Ravasi, D., Mangili, F., Huber, D., Azzimonti, L., Engeler, L., Vermes, N., ... & Flacio, E. (2022). Risk-
718 based mapping tools for surveillance and control of the invasive mosquito *Aedes albopictus* in
719 Switzerland. *International Journal of Environmental Research and Public Health*, 19(6), 3220.
720
- 721 Ravasi, D., Parrondo Monton, D., Tanadini, M., & Flacio, E. (2021). Effectiveness of integrated *Aedes*
722 *albopictus* management in southern Switzerland. *Parasites & vectors*, 14(1), 1-15.
723
- 724 Rezza G, Nicoletti L, Angelini R, Romi R, Finarelli AC, Panning M, et al. Infection with chikungunya
725 virus in Italy: an outbreak in a temperate region. *Lancet*. 2007;370:1840–6. [https://doi.org/10.1016/S0140-6736\(07\)61779-6](https://doi.org/10.1016/S0140-6736(07)61779-6).
726
727
- 728 Roche, B., Léger, L., L'Ambert, G., Lacour, G., Foussadier, R., Besnard, G., ... & Fontenille, D.
729 (2015). The spread of *Aedes albopictus* in metropolitan France: contribution of environmental drivers
730 and human activities and predictions for a near future. *PloS one*, 10(5), e0125600.
731
- 732 Roiz, D., Neteler, M., Castellani, C., Arnoldi, D., & Rizzoli, A. (2011). Climatic factors driving invasion
733 of the tiger mosquito (*Aedes albopictus*) into new areas of Trentino, northern Italy. *PloS one*, 6(4),
734 e14800.
735
- 736 Roiz, D., Rosà, R., Arnoldi, D., & Rizzoli, A. (2010). Effects of temperature and rainfall on the activity
737 and dynamics of host-seeking *Aedes albopictus* females in northern Italy. *Vector-borne and zoonotic*
738 *diseases*, 10(8), 811-816.
739
- 740 Romiti, F., Casini, R., Magliano, A., Ermenegildi, A., & De Liberato, C. (2022). *Aedes albopictus*
741 abundance and phenology along an altitudinal gradient in Lazio region (central Italy). *Parasites &*
742 *Vectors*, 15(1), 1-11.
743
- 744 Romiti, F., Ermenegildi, A., Magliano, A., Rombolà, P., Varrenti, D., Giammattei, R., ... & De Liberato,
745 C. (2021). *Aedes albopictus* (Diptera: Culicidae) monitoring in the Lazio region (central Italy). *Journal*
746 *of Medical Entomology*, 58(2), 847-856.
747

- 748 Rosà, R., Marini, G., Bolzoni, L., Neteler, M., Metz, M., Delucchi, L., ... & Rizzoli, A. (2014). Early
 749 warning of West Nile virus mosquito vector: climate and land use models successfully explain
 750 phenology and abundance of *Culex pipiens* mosquitoes in north-western Italy. *Parasites & vectors*, 7,
 751 1-12.
- 752
- 753 Schaffner, U., Steinbach, S., Sun, Y., Skjøth, C. A., de Weger, L. A., Lommen, S. T., ... & Müller-
 754 Schärer, H. (2020). Biological weed control to relieve millions from *Ambrosia* allergies in Europe.
 755 *Nature Communications*, 11(1), 1745.
- 756
- 757 Sillero, N. and Barbosa, A. M. (2020). Common mistakes in ecological niche models. *International*
 758 *Journal of Geographical Information Science*, pages 1–14.
- 759
- 760 Tisseuil, C., Velo, E., Bino, S., Kadriaj, P., Mersini, K., Shukullari, A., ... & Gilbert, M. (2018).
 761 Forecasting the spatial and seasonal dynamic of *Aedes albopictus* oviposition activity in Albania and
 762 Balkan countries. *PLoS Neglected Tropical Diseases*, 12(2), e0006236.
- 763
- 764 Tjaden, N. B., Thomas, S. M., Fischer, D., & Beierkuhnlein, C. (2013). Extrinsic incubation period of
 765 dengue: knowledge, backlog, and applications of temperature dependence. *PLoS neglected tropical*
 766 *diseases*, 7(6), e2207.
- 767
- 768 Toma L, Severini F, Di Luca M, Bella A, Romi R. 2003 Seasonal patterns of oviposition and egg
 769 hatching rate of *Aedes albopictus* in Rome. *J. Am. Mosq. Control Assoc.* 19, 19–22.
- 770
- 771 Torina, A., La Russa, F., Blanda, V., Peralbo-Moreno, A., Casades-Martí, L., Di Pasquale, L., ... &
 772 Ruiz-Fons, F. (2023). Modelling time-series *Aedes albopictus* abundance as a forecasting tool in
 773 urban environments. *Ecological Indicators*, 150, 110232.
- 774
- 775 Tran, A., L'ambert, G., Lacour, G., Benoît, R., Demarchi, M., Cros, M., ... & Ezanno, P. (2013). A
 776 rainfall-and temperature-driven abundance model for *Aedes albopictus* populations. *International*
 777 *journal of environmental research and public health*, 10(5), 1698-1719.
- 778
- 779 Venturi G, Di Luca M, Fortuna C, Remoli ME, Riccardo F, Severini F, et al. Detection of a
 780 chikungunya outbreak in central Italy, August to September 2017. *Euro Surveill.* 2017;22:17–00646.
 781 [https:// doi. org/ 10. 2807/ 1560-7917. es. 2017. 22. 39. 17- 00646.](https://doi.org/10.2807/1560-7917.es.2017.22.39.17-00646)
- 782
- 783 Wolpert, D.H. (1992). Stacked generalization. *Neural Networks* 5(2):241-259
- 784
- 785 Zink, K., Vogel, H., Vogel, B., Magyar, D., & Kottmeier, C. (2012). Modeling the dispersion of
 786 *Ambrosia artemisiifolia* L. pollen with the model system COSMO-ART. *International journal of*
 787 *biometeorology*, 56, 669-680.
- 788
- 789 Zhou Z. H. (2012). Ensemble methods: foundations and algorithms. Boca Raton: Chapman and
 790 Hall/CRC.

791 Supplementary materials 1

792 1.1. Environmental Covariates

793 We selected three main environmental drivers that can significantly influence the
794 behaviour and development of mosquitoes, namely temperature, photoperiod and
795 precipitation (Toma et al., 2003; Becker et al., 2010; Roiz et al., 2010, 2011; Romiti et al.,
796 2021; Carrieri et al., 2023).

797 As ectothermic organisms, warmer temperatures generally promote faster
798 development and increase the overall metabolic rate of mosquitoes, leading to shorter life
799 cycles and higher population growth rates (Delatte et al., 2009; Pumpuni et al., 1992;
800 Waldock et al., 2013; Marini et al., 2020). We downloaded the ERA5Land (Muñoz-Sabater et
801 al., 2021) dataset representing the hourly gridded estimate of mean temperature over
802 Europe for the period 2010-2022 and computed the weekly median temperature for each
803 grid cell using the R function `terra::app()` (Hijmans 2023). By aggregating weekly, we
804 observed that the aggregated values tended to be relatively high during the European colder
805 months (November-February). To better capture the seasonality of mosquito phenology and
806 avoid predicting oviposition during the winter season, a threshold-like variable was created
807 by setting all temperature values below 15 °C to zero. By applying this modification,
808 temperatures below 15 °C were essentially associated with zero or low egg abundance. This
809 manipulation helps ensure that the model focuses on the temperature conditions more
810 relevant to mosquito activity and development, which are typically associated with warmer
811 periods. Applying this modification to temperature might appear as a strong assumption,
812 given that *Ae. albopictus* is capable of completing its life cycle and surviving within a wide
813 temperature range (Reinhold, Lazzari and Lahondère, 2018). However, several studies
814 suggest that the optimal temperature range to complete the life cycle lies between 15 °C and
815 35 °C, even though the lower developmental zero temperature for this species is reported to
816 be around 10.4 °C (Reinhold, Lazzari and Lahondère, 2018 and reference therein; Marini et
817 al., 2020; Petrić et al., 2021 and reference therein). Considering this biological evidence,
818 setting a temperature threshold of 15 °C in the analysis aligns with the findings that *Ae.*
819 *albopictus* optimal development and activity are more favourable within this temperature
820 range (Marini et al., 2020).

821 Photoperiod refers to the duration of daylight in 24 hours. It plays a crucial role in
822 regulating mosquito behaviour, particularly concerning their activity, feeding patterns, the
823 timing of mating and egg-laying behaviours (Pumpuni et al., 1992). In fact, in the temperate
824 strain of *Ae. albopictus*, changes in the photoperiod length trigger the laying of cold-resistant
825 eggs commonly referred to as “diapausing eggs” (Thomas et al., 2012; Urbanski et al., 2012;
826 Lacour et al., 2015; Diniz et al., 2017). Diapause refers to an insect species' evolutionary
827 adaptation to overcome poor environmental conditions by passing through an alternate and
828 inactive physiological stage. In the case of *Ae. albopictus*, the maternal photoperiod
829 experienced at pupal and adult stage is the environmental stimulus implied to induce
830 oviposition of “diapausing eggs” (Lacour et al., 2015). To account for the yearly variation in
831 the weekly photoperiod length, we computed the daily photoperiod for each 9 x 9 km grid cell
832 between 2010 and 2022 using the R function `geosphere::photoperiod()` (Hijmans
833 2021) and then computed the weekly median.

834 Precipitation is another environmental factor that can influence mosquito populations
835 and their behaviour, as mosquitoes require standing water for their larvae to develop (Becker

836 et al., 2010; Roiz et al., 2010). Precipitation events can create or replenish breeding sites for
 837 mosquitoes, while heavy rain or storms can flush out eggs and larvae from the breeding
 838 sites or temporarily disrupt mosquito flying activity due to the impact of raindrops and
 839 unfavourable flight conditions (Koenraadt and Harrington, 2008; Caldwell et al., 2021). We
 840 downloaded the ERA5Land (Muñoz-Sabater et al., 2021) dataset representing the hourly
 841 gridded estimate of precipitation over Europe for the period 2010-2022 and computed the
 842 weekly cumulative sum for each grid cell using the R function `terra::app()` (Hijmans
 843 2023).

844 For each of these three variables, we considered lagged values of these factors as
 845 well, since the mosquito life cycle can take several days or weeks to complete (Becker et al.,
 846 2010; Roiz et al., 2010). The lagged temperatures and photoperiod were calculated as the
 847 median value between the temperatures recorded in the current week (i), the previous week
 848 (i-1), and the week before that (i-2), whilst the lagged precipitation was computed as the
 849 cumulative value between the precipitation recorded in the current week (i), the previous
 850 week (i-1), and the week before that (i-2).

851

852 1.2 Explorative analysis and model building

853 We carried out an explorative analysis on a subset of the aggregated ovitraps to
 854 understand which are the main predictors to include in the stacked model. The subset of the
 855 aggregated ovitraps (n = 20) was randomly selected but with the constraint of having at least
 856 three years of observations.

857 The graphical inspection of the aggregated observations showed a regular pattern repeating
 858 approximately every year. Additionally, within any year, there are two sub-periods,
 859 disentangling the cold period (where no eggs are generally reported), from the warmer
 860 period, spanning from spring to fall, where the number of recorded eggs has a magnitude
 861 that seems affected by other factors than the seasonality. Therefore, we tested for
 862 environmental drivers associated with the species' biology (temperature, photoperiod, and
 863 precipitation), that influenced the time evolution of the observed eggs.

864 We included the seasonal and environmental variables in a regression model with
 865 autoregressive errors of order one, i.e. for the fitting we use the ordinary least squares (OLS)
 866 with AR(1) errors. We have attempted to capture the seasonality by employing Fourier's
 867 harmonics sine and cosine waves, with four waves in total. One pair of sine and cosine
 868 waves is responsible for capturing the annual pattern, while the other pair is utilized to
 869 account for the seasonality within a given year. Concerning the environmental predictors, we
 870 tested the inclusion of both weekly and weekly-lagged values (e.g. the median temperature
 871 recorded two and three weeks ago).

872 The model's structure with different predictors and lags was fitted on different
 873 aggregated ovitraps, and the best model formulation, i.e. that one displaying
 874 overall goodness of fit (in sample) $R^2_{adjusted} \sim 0.75$ and equally good forecast
 875 performance (out of sample), was selected as that one inferring the number of eggs as a
 876 function of temperature, photoperiod, and precipitation, all lagged by -2 and -3 weeks, the
 877 four Fourier's harmonics, and an autoregressive component based on the number of eggs
 878 observed at week t-1. The residuals from model fitting were approximately Gaussian in all
 879 cases.

880 The benefit of selecting the error term as AR(1) was two-fold: the residuals are mostly
 881 uncorrelated and with such parameterization, it is possible to rewrite the model as a genuine
 882 regression model, so the cross-validation requires minimum adjustments, and stacking

883 computing routines are readily available. Further generalisation to more involved ARMA
884 errors seemed to provide no extra benefit in terms of goodness of fit, and do not share the
885 same representation as the OLS-AR(1), making the cross-validation harder to implement
886 and trust.

887

Supplementary materials 2

888

889

2.1 Hyperparameters tuning

890 In machine learning, hyperparameters tuning is the process of selecting the optimal
 891 settings for configuration parameters that are not learned from the data. It is a crucial task
 892 because it improves model performance, avoids overfitting or underfitting, adaptability to
 893 different datasets, and generalisation to new data. For each algorithm, a hyperparameter
 894 space was defined and the tuning was conducted using a random search strategy with a 10-
 895 fold cross-validation. Due to computational constraints, we chose only specific
 896 hyperparameters to conduct the tuning, while for the remaining ones, the values are set to
 897 default. The hyperparameter space by algorithms is shown in Tab. S2.1.

898

899 **Table S2.1:** Hyperparameter space for the analysed algorithms

Algorithm	Hyperparameter	Type	Lower	Upper
Boosted Regression Trees (BRT)				
	n.trees	integer	200	10000
	interaction depth	integer	1	5
	cv folds	integer	5	15
Cubist				
	committees	integer	1	10
Extreme Gradient Boosting (XGBoost)				
	nrounds	integer	10	30
	max depth	integer	4	10
	eta	numeric	0.2	0.4
	subsample	numeric	0.9	1
	min child weight	integer	1	4
	colsample by tree	numeric	0.5	0.6
Random Forest (RF)				
	n.trees	integer	200	500
	mtry	integer	4	7

min node size	integer	5	10
---------------	---------	---	----

901 2.2 Stacked models parameters and summary results

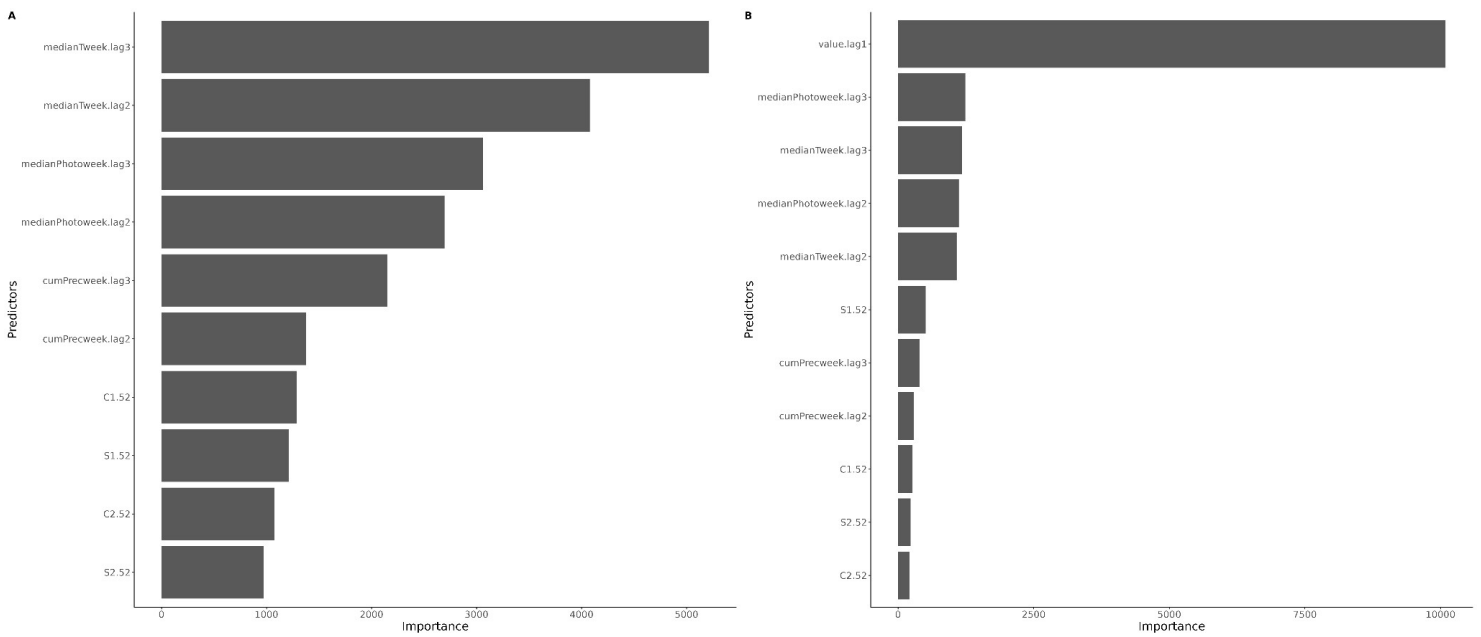
902

903 **Tab. S2.2** Parameters of the ensemble models

904

	Regression model		Autoregressive model	
	Estimate (SE)	P-value	Estimate (SE)	P-value
<i>Intercept</i>	0.854 (0.401)	p < 0.05	1.14 (0.239)	p < 0.05
<i>xgBoost</i>	-0.002 (0.014)	p = 0.874	-0.055 (0.014)	p < 0.05
<i>RF</i>	0.722 (0.016)	p < 0.05	0.056 (0.017)	p < 0.05
<i>GBM</i>	-0.068 (0.011)	p < 0.05	0.226 (0.009)	p < 0.05
<i>Cubist</i>	0.371 (0.017)	p < 0.05	0.782 (0.015)	p < 0.05

905



907 **Fig. S2.3** Variable importance of the random forest base learner for the two model
 908 formulations: A) regression model and B) autoregressive model.

909

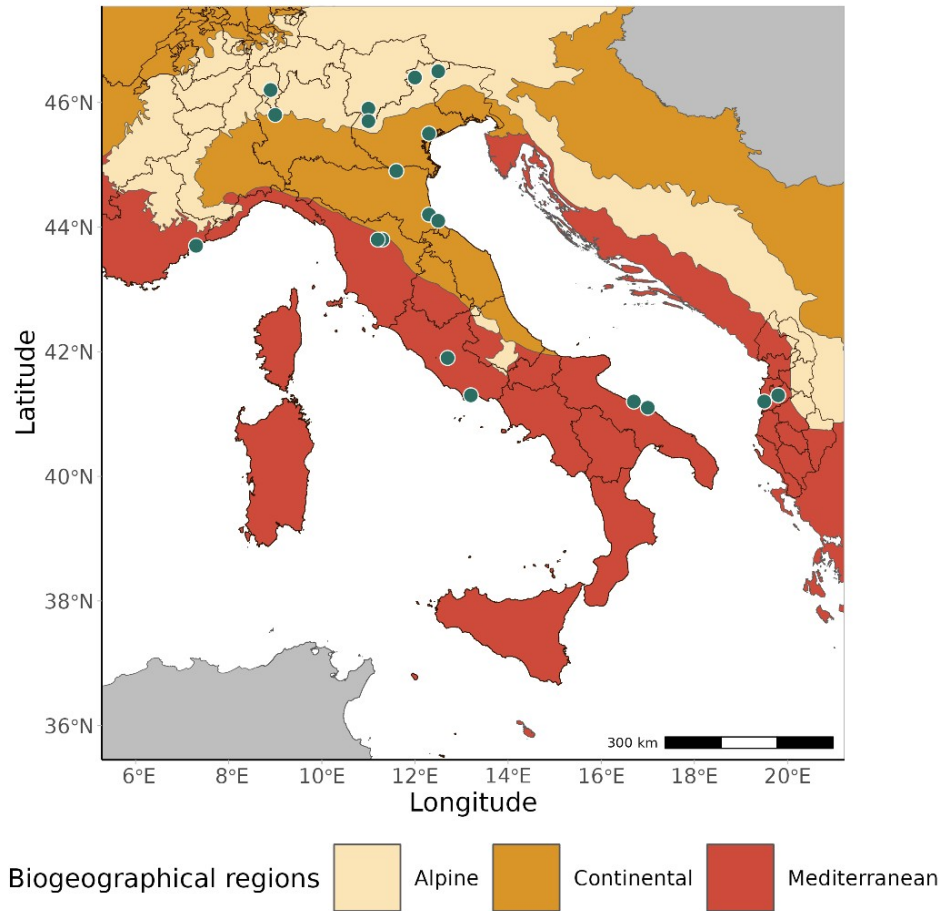
910

911

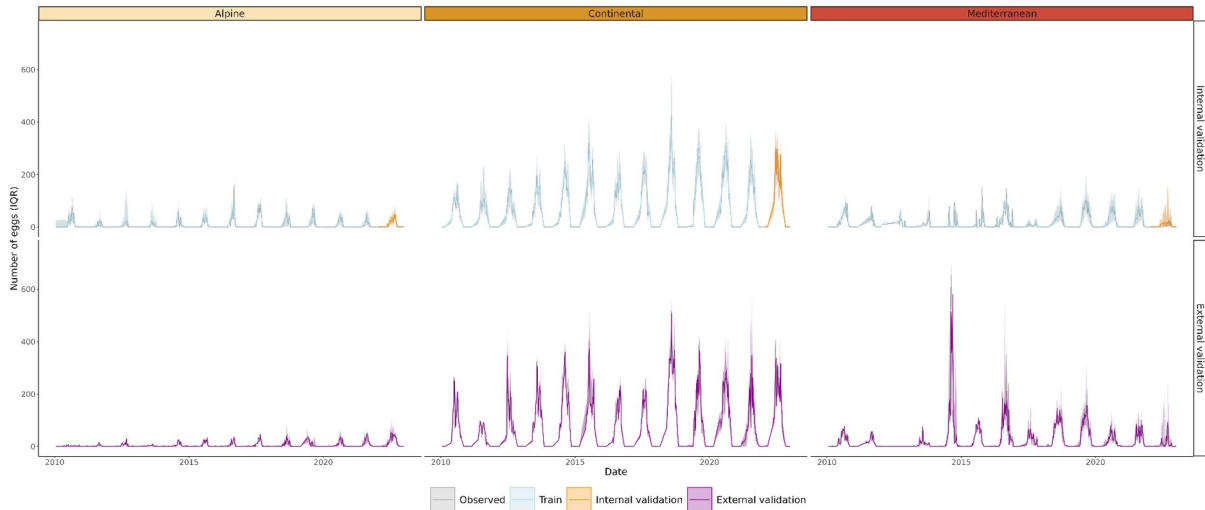
912 Supplementary materials 3

913

914 Internal and external validations

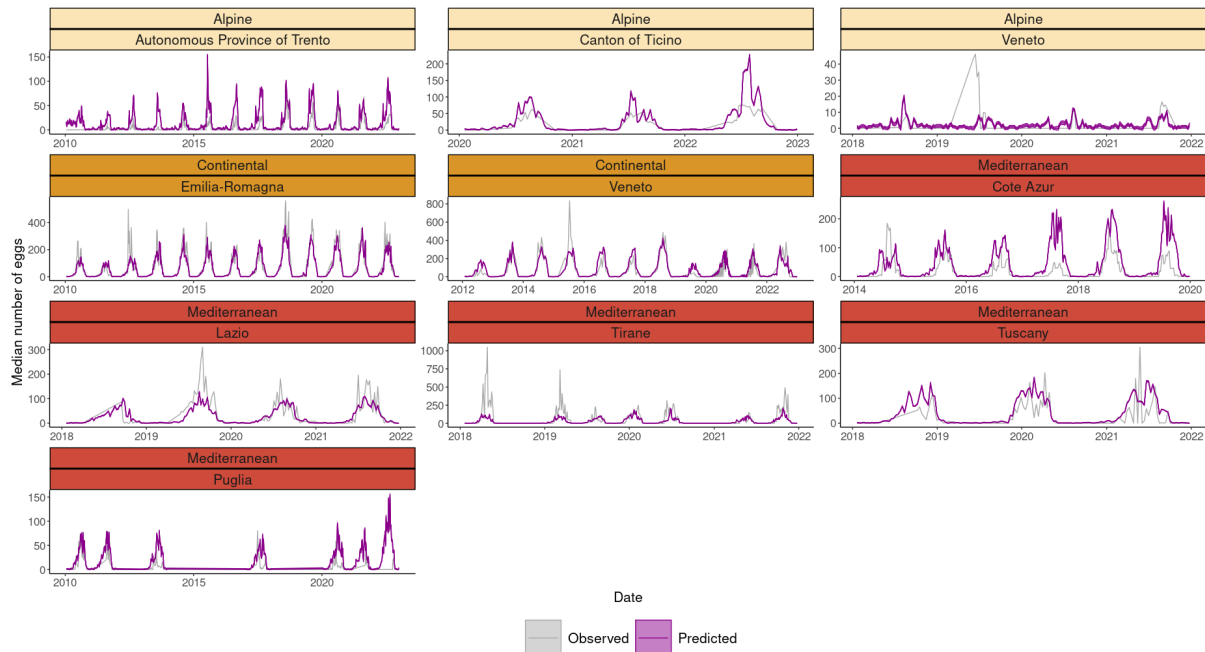
916 **Fig. S3.1** Location of the aggregated ovitraps employed for the external validation.

917



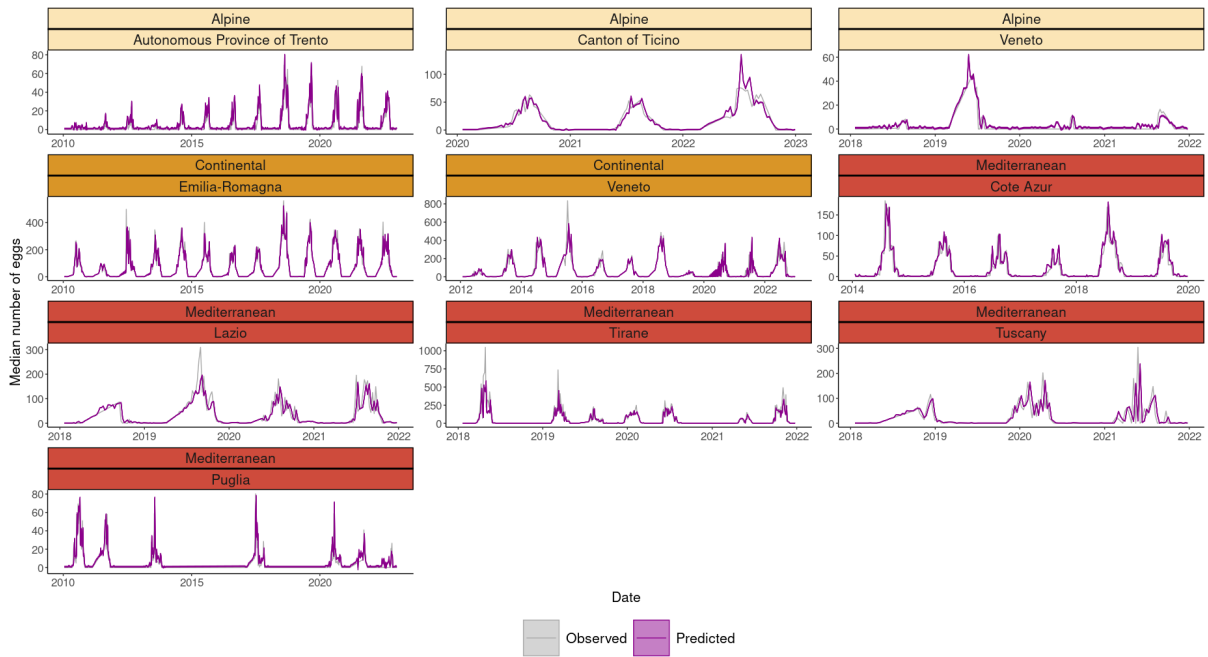
918
919
920
921
922
923
924
925
926

Fig. S3.2. The median and interquartile range of the number of eggs observed (grey lines), and predicted by the autoregressive model in both the internal and external validation. Both the observed and predicted values were aggregated over the three biogeographical regions to allow an easier representation.



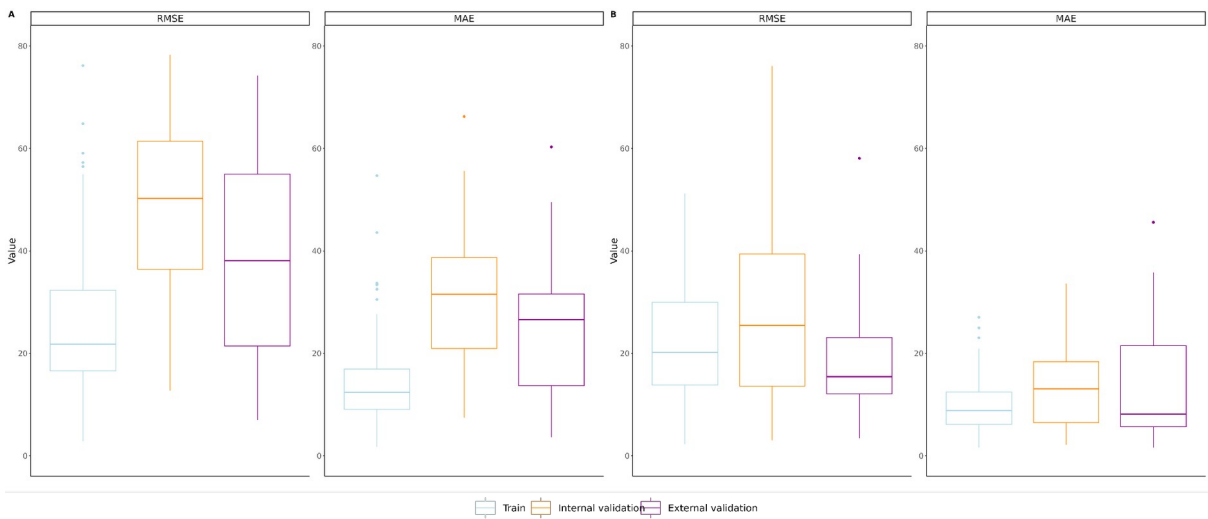
927
928
929
930
931
932

Fig. S3.3 The median and interquartile range of the number of eggs observed (grey lines) and predicted by the regression model in external validation. Both the observed and predicted values were aggregated over the NUTS2 levels to allow an easier representation.

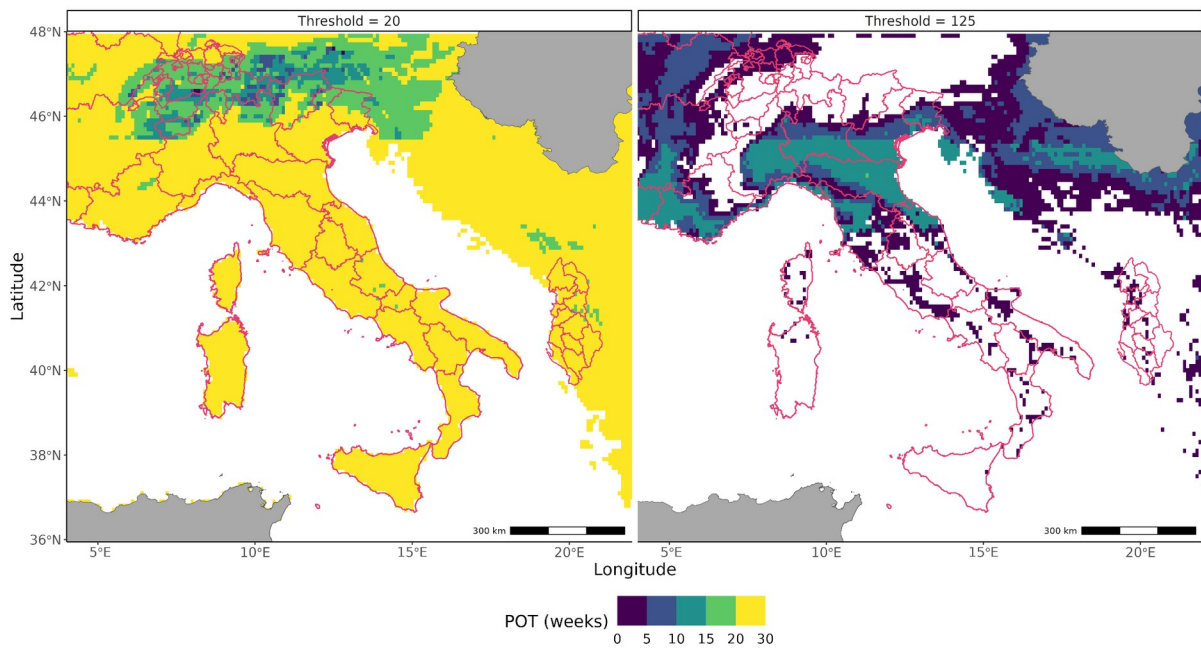


933
 934 **Fig. S3.4** The median and interquartile range of the number of eggs observed (grey lines)
 935 and predicted by the autoregressive model in external validation. Both the observed and
 936 predicted values were aggregated over the NUTS2 levels to allow an easier representation.

937
 938



939
 940 **Fig. S3.5** Root mean squared error (RMSE) and mean absolute error (MAE) for the A)
 941 regression model (Eq. 1) and B) autoregressive model formulation (Eq. 2).



942
 943 **Fig. S3.6.** Spatial representation of the interquartile range of period-over-threshold (POT)
 944 length for the year 2022 over the area of interest.

945

946 **Tab. S3.7** Estimates coefficients and statistics of the period-over-threshold model (GLM with
 947 Poisson error).

948

	Observed		Predicted	
	Estimate (SE)	P-value	Estimate (SE)	P-value
Intercept	47.943 (27.718)	(p = 0.084)	-361.983 (1.018)	(p < 0.05)
year	-0.023 (0.014)	(p = 0.097)	0.18 (0.001)	(p < 0.05)
bgrContinental	-98.28 (29.559)	(p < 0.05)	318.68 (1.268)	(p < 0.05)
bgrMediterranean	-81.904 (36.298)	(p < 0.05)	263.636 (1.2)	(p < 0.05)
year:bgrContinental	0.049 (0.015)	(p < 0.05)	-0.157 (0.001)	(p < 0.05)
year:bgrMediterranean	0.041 (0.018)	(p < 0.05)	-0.13 (0.001)	(p < 0.05)

949

950 References of Supplementary Materials

- 951 Becker, N., Petric, D., Zgomba, M., Boase, C., Madon, M., Dahl, C., & Kaiser, A. (2010). Mosquitoes
952 and their control. Springer Science & Business Media.
953
- 954 Caldwell, J. M., LaBeaud, A. D., Lambin, E. F., Stewart-Ibarra, A. M., Ndenga, B. A., Mutuku, F. M., ...
955 & Mordecai, E. A. (2021). Climate predicts geographic and temporal variation in mosquito-borne
956 disease dynamics on two continents. *Nature communications*, 12(1), 1233.
957
- 958 Carrieri, M., Albieri, A., Angelini, P., Soracase, M., Dottori, M., Antolini, G., & Bellini, R. (2023). Effects
959 of the Weather on the Seasonal Population Trend of *Aedes albopictus* (Diptera: Culicidae) in Northern
960 Italy.
961
- 962 Delatte, H., Gimonneau, G., Triboire, A., & Fontenille, D. (2009). Influence of temperature on
963 immature development, survival, longevity, fecundity, and gonotrophic cycles of *Aedes albopictus*,
964 vector of chikungunya and dengue in the Indian Ocean. *Journal of medical entomology*, 46(1), 33-41.
965
- 966 Diniz, D. F. A., de Albuquerque, C. M. R., Oliva, L. O., de Melo-Santos, M. A. V., & Ayres, C. F. J.
967 (2017). Diapause and quiescence: dormancy mechanisms that contribute to the geographical
968 expansion of mosquitoes and their evolutionary success. *Parasites & vectors*, 10, 1-13.
969
- 970 Hijmans R (2023). terra: Spatial Data Analysis. R package version 1.7-28, [https://CRAN.R-](https://CRAN.R-project.org/package=terra)
971 [project.org/package=terra](https://CRAN.R-project.org/package=terra)
972
- 973 Hijmans R (2021). geosphere: Spherical Trigonometry_. R package version 1.5-14, [https://CRAN.R-](https://CRAN.R-project.org/package=geosphere)
974 [project.org/package=geosphere](https://CRAN.R-project.org/package=geosphere)
975
- 976 Koenraadt, C. J. M., & Harrington, L. C. (2008). Flushing effect of rain on container-inhabiting
977 mosquitoes *Aedes aegypti* and *Culex pipiens* (Diptera: Culicidae). *Journal of medical entomology*,
978 45(1), 28-35.
979
- 980 Marini, G., Manica, M., Arnoldi, D., Inama, E., Rosà, R., & Rizzoli, A. (2020). Influence of temperature
981 on the life-cycle dynamics of *Aedes albopictus* population established at temperate latitudes: A
982 laboratory experiment. *Insects*, 11(11), 808.
983
- 984 Muñoz-Sabater J, Dutra E, Agustí-Panareda A, Albergel C, Arduini G, Balsamo G, Boussetta S,
985 Choulga M, Harrigan S, Hersbach H, et al. ERA5-Land: A state-of-the-art global reanalysis dataset for
986 land applications. *Earth Syst Sci Data Discuss* 2021: 1–50.
987
- 988 Lacour, G., Chanaud, L., L'Ambert, G., & Hance, T. (2015). Seasonal synchronization of diapause
989 phases in *Aedes albopictus* (Diptera: Culicidae). *PloS one*, 10(12), e0145311.
990
- 991 Petrić, M., Ducheyne, E., Gossner, C. M., Marsboom, C., Venail, R., Hendrickx, G., & Schaffner, F.
992 (2021). Seasonality and timing of peak abundance of *Aedes albopictus* in Europe: Implications to
993 public and animal health. *Geospatial Health*, 16(1).
994
- 995 Pumpuni, C. B., Knepler, J., & Craig Jr, G. B. (1992). Influence of temperature and larval nutrition on
996 the diapause inducing photoperiod of *Aedes albopictus*. *Journal of the American Mosquito Control*
997 *Association*, 8(3), 223-227.
- 998 Reinhold, J. M., Lazzari, C. R., & Lahondère, C. (2018). Effects of the environmental temperature on
999 *Aedes aegypti* and *Aedes albopictus* mosquitoes: a review. *Insects*, 9(4), 158.

- 1000
1001 Roiz, D., Neteler, M., Castellani, C., Arnoldi, D., & Rizzoli, A. (2011). Climatic factors driving invasion
1002 of the tiger mosquito (*Aedes albopictus*) into new areas of Trentino, northern Italy. *PloS one*, 6(4),
1003 e14800.
1004
1005 Roiz, D., Rosà, R., Arnoldi, D., & Rizzoli, A. (2010). Effects of temperature and rainfall on the activity
1006 and dynamics of host-seeking *Aedes albopictus* females in northern Italy. *Vector-borne and zoonotic*
1007 *diseases*, 10(8), 811-816.
1008
1009 Romiti, F., Ermenegildi, A., Magliano, A., Rombolà, P., Varrenti, D., Giammattei, R., ... & De Liberato,
1010 C. (2021). *Aedes albopictus* (Diptera: Culicidae) monitoring in the Lazio region (central Italy). *Journal*
1011 *of Medical Entomology*, 58(2), 847-856.
1012
1013 Thomas, S. M., Obermayr, U., Fischer, D., Kreyling, J., & Beierkuhnlein, C. (2012). Low-temperature
1014 threshold for egg survival of a post-diapause and non-diapause European aedine strain, *Aedes*
1015 *albopictus* (Diptera: Culicidae). *Parasites & vectors*, 5(1), 1-7.
1016
1017 Toma L, Severini F, Di Luca M, Bella A, Romi R. 2003 Seasonal patterns of oviposition and egg
1018 hatching rate of *Aedes albopictus* in Rome. *J. Am. Mosq. Control Assoc.* 19, 19–22.
1019
1020 Urbanski, J., Mogi, M., O'Donnell, D., DeCotiis, M., Toma, T., & Armbruster, P. (2012). Rapid adaptive
1021 evolution of photoperiodic response during invasion and range expansion across a climatic gradient.
1022 *The American Naturalist*, 179(4), 490-500.
1023
1024 Waldock, J., Chandra, N. L., Lelieveld, J., Proestos, Y., Michael, E., Christophides, G., & Parham, P.
1025 E. (2013). The role of environmental variables on *Aedes albopictus* biology and chikungunya
1026 epidemiology. *Pathogens and global health*, 107(5), 224-241.